*Egypt. J. Chem.* **Vol. 68**, No. 11 pp. 1 - 23 (2025)

**Egyptian Journal of Chemistry**

**http://ejchem.journals.ekb.eg/**

# Recent Update on Using Metal Organic Framework for Uptake of Pesticides from Wastewater

**Ahmed M. Mansour[a], Hassan Abdel-Gawad [b*], Soha F. Mohammed[a], Kareem A. Asla[a] and Reda M. Abdelhameed[b]**

*[a]Chemistry Department, Faculty of Science, Zagazig University, Zagazig, Egypt*

*[b]Applied Organic Chemistry Department, Chemical Industries Research Institute, National Research Centre, Dokki, Giza, Egypt*

**Abstract**

Pesticides are widely used to manage plant diseases and pests; however, their contamination of soil and water raises serious health and environmental concerns, including a potential link to diabetes and cancer. They fall into four main categories: organochlorines, organophosphates, carbamates, and synthetic pyrethroids. Addressing pesticide pollution, particularly from wastewater, is essential for environmental sustainability. Effective removal techniques, such as biodegradation, electrochemical processes, and adsorption, can achieve 99.9% efficiency, which is pivotal due to their simplicity and cost-effectiveness. Metal-Organic Frameworks (MOFs) are emerging as superior sorbents for pesticide removal, outpacing traditional materials in adsorption capacity and stability. These structures, formed by metal ions and organic linkers, possess large surface areas and high porosity, making them versatile for applications in clean energy, gas storage, and various technological advancements. Recent developments in integrating carbonaceous compounds and nanoparticles have further enhanced the functionality of MOFs, enabling diverse synthesis methods that broaden their applicability in technology and environmental remediation efforts.

**Keywords**: Pesticides; Removal; Metal-Organic Frameworks; Wastewater.

**Abbreviations**

MOFs= Metal-Organic Frameworks; OPs=Organophosphate pesticides;UIO=University of Oslo;ZIFs =Zeoliticimidazolate framework.

**Table of contents**



## 1. Introduction

Pesticides are widely used throughout the world to control plant diseases and keep pests away from crops. But because pesticides pollute soil and water, they cause serious health and environmental problems, including diabetes, cancer, and a host of other diseases that impact people, animals, plants, and birds[1]. Pesticides can be classified into four primary categories based on their chemical structure: organochlorines, organophosphates, carbamates, and synthetic pyrethroids. Organochlorines, which encompass compounds such as DDT and chlordane, are distinguished by their chlorine content and are employed against a wide range of insects by inducing convulsions and paralysis. Organophosphates, derived from phosphoric acid, function by inhibiting cholinesterase, an enzyme vital for nerve function in insects, with examples including Malathion and chlorpyrifos. This category is noted for its moderate resistance to pests and biodegradability, contributing to reduced pollution. Their residues were detected in fruits, vegetables and tea leaves [2-4]. Carbamates, like organophosphates

*Corresponding author e-mail: abdelgawadhassan@hotmail.com.; (Hassan Abdel-Gawad).
Received date 01 June 2025; Revised date 15 July 2025; Accepted date 22 July 2025
DOI: 10.21608/ejchem.2025.391269.11858

in mechanism but differing in structure, tend to degrade more rapidly in the environment, with compounds like carbaryl and methomyl. Synthetic pyrethroids mimic natural pyrethrins and are favoured for food safety due to their rapid breakdown in light exposure[5]. Additionally, neonicotinoids, triazines, chloroacetanilides, and chlorophenoxy derivatives are classes of pesticides. Recent works for MOF in adsorption of pesticides during water treatment were investigated [6-11].

Developing techniques to protect the environment and remove environmental pollution, especially wastewater derived from pesticide pollution, is therefore of vital importance from a sustainability perspective. Numerous techniques have demonstrated effective pesticide removal, including biodegradation, electrochemical methods, ultrasound, oxidative degradation, photocatalysis[12, 13], and adsorption. Among these, adsorption is particularly effective for capturing trace levels of pesticides from wastewater, achieving an adsorption rate of up to 99.9%. Its advantages include ease of operation, simple design, low energy consumption, and cost-effectiveness [14]. Although various sorbents have been utilized for pesticide determination and removal, they often exhibit significant limitations. An effective adsorbent requires high adsorption capacity, and Metal-Organic Frameworks (MOFs) stand out in this regard. MOFs not only have high adsorption capabilities but also demonstrate remarkable chemical and physical stability, ultrahigh porosity, and a variety of other useful properties[15].MOFs, as defined by Yaghi et al., are permeable structures created when metal ions co-ordinately interact with bridging ligands or organic linkers to form constructions with pores. Metal-Organic Frameworks (MOFs) represent a diverse family of crystalline materials characterized by their large internal surface area and impressive porosity, reaching up to 90% free volume and surface areas as high as 6000 m²/g. These exceptional attributes, along with the diversity of their inorganic and organic components, make MOFs promising options for clean energy applications, especially as high-capacity adsorbents for separation procedures and gas storage (e.g., $H_2$, $CH_4$). The scope of MOFs has expanded to include uses in membrane technology, thin-film electronics, catalysis, and biological imaging. Recent advancements have seen the incorporation of carbonaceous compounds, composite materials, and nanoparticles into MOFs to enhance their functionality and stability in various environments [16-18]. MOFs can have a variety of forms and structures, including linear, pentagonal bipyramidal, trigonal-prismatic, and others, depending on the ligand and ions utilized[15]. Several techniques, including mechanochemical, electrochemical, diffusion, solvothermal, microwave-assisted, and ultrasound approaches, have been used for the synthesis of MOFs[19].

## 2. Pesticide uptakes with MOFs

### 2.1. Removal of organophosphate pesticides

Cu-BTC@cotton was prepared by immersing the oxidized cotton material in ethanol that had varying amounts of Cu-BTC. The so-prepared Cu-BTC@cotton composite has been effectively created as a new adsorbent for the efficient elimination of ethion, which is an OP insecticide, from water. Ethion's organophosphorus pesticide adsorption onto Cu–BTC@cotton composite was thoroughly investigated. Both the Cu of MOF and the binding sites of the composite, which were represented by the cellulose functional groups, were connected to ethion via sulfur. The elimination percentage of ethion exceeded 97%, and the Cu-BTC@cotton composite showed the highest sorption capacity of about 182 mg/g (Figure 1). The adsorption efficiency of the Cu–BTC@cotton composite remained excellent and exceeded 85% even after five recycling cycles[20].

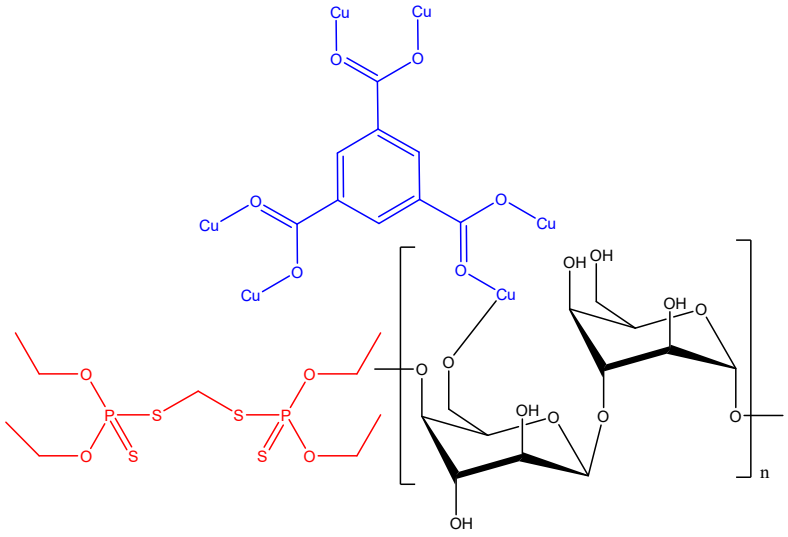


**Figure 1**: Cellulose incorporated Cu-BTC MOF for removal of ethion pesticide

Zr-MOF@Ox-cotton was successfully synthesized by the interaction of Cotton fabrics with oxalyl chloride. The so-called hybrid was used to remove diazinon and chlorpyrifos as pesticides from wastewater. Diazinon and chlorpyrifos adsorption onto the hybrid followed the Langmuir profile and pseudo-second order model. Maximum adsorption capacities of diazinon and chlorpyrifos onto the hybrid were 464.69 and 389.69 mg/g, respectively. Physical deposition onto the pores of hybrid materials and a variety of chemical interactions, such as electrostatic, coordination, hydrogen, and π-π interactions, were thought to be the adsorption mechanism (Figure 2)[21].

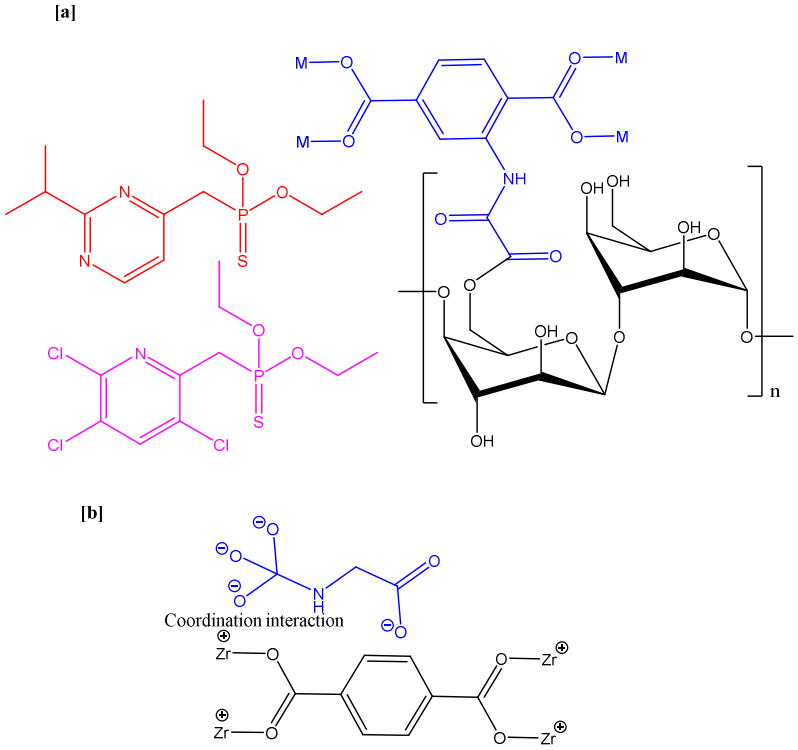


**Figure 2: [a]** Mechanism of Chlorpyrifos and Diazinon Adsorption onto MOF@Ox-cotton hybrid; [b] Adsorption of OP pesticide onto Zr-MOFs

The $^{14}$C-ethion pesticide was effectively removed from wastewater using Cu-BTC as an adsorbent. Cu-BTC removed 94% of the $^{14}$C-ethion from aqueous solution with an adsorption capability of about 122 mg/g. Six distinct forms of interactions between adsorbates and MOFs active sites are thought to be responsible for the uptake mechanism of $^{14}$C-ethion by Cu-BTC. These interactions include complex formation, hydrogen bonding, π–π interaction, acid–base interaction, electrostatic interaction, and adsorption based on hydrophobic interactions. The adsorption kinetics of the pesticide removal over time could be accurately represented by a pseudo-first-order model[22].

ZIF-67(Co) and ZIF-8 (Zn) were utilized to get rid of two popular pesticides, ethion and prothiofos.The adsorption capacities of ZIF-67 approached 210.8 mg/g for ethion and 261.1 mg/g for prothiofos. Whereas the adsorption capacities of ZIF-8 were 279.3 mg/g and 366.7 mg/g for ethion and prothiofos, respectively. According to kinetic investigations, the pseudo-second-order model best suited the elimination of both ethion and prothiofos by ZIFs.The Langmuir model best described the adsorption process, suggesting that pesticide adsorption took place on the ZIFs surface as a monolayer adsorbent. The interaction of prothiofos and ethion insecticides with the metal ions (Zn/Co) of ZIFs surface in dry and aqueous solution was the primary cause of the adsorption mechanism, according to MC and MD simulations. Additionally, the formation of hydrogen bonds with ZIF-8/67's imidazolium stabilized this interaction[23].

UIO-66 and UIO-67 were successfully developed to remove dichlorvos and metrifonate from aqueous solutions. The highest adsorption capacities of Dichlorvos and Metrifonate by UiO-67 are determined to be 571.43 mg/g and 378.78 mg/g, respectively, while the highest adsorption capacities of Dichlorvos and Metrifonate by UIO-66 are determined to be 172.4 mg/g and 52.71 mg/g.UIO-67 has higher adsorption capabilities for dichlorvos and metrifonate due to its bigger pores and higher number of Zr OH.The Langmuir and pseudo-second-order models provided an accurate description of the isotherm and kinetic data[24].

NU-1000 and UiO-67 were synthesized for the uptake of glyphosate from the aqueous media. Glyphosate had a greater adsorption capacity on NU-1000 (1516 mg/g) than on UiO-67 (1335 mg/g). The higher adsorption efficiency of NU-1000 may be because of its bigger pore diameters and higher interaction energy (−37.63 KJ) of glyphosate with its nodes. The adsorption process is better explained by the pseudo second order model, according to the adsorption kinetic studies[25].
W. Li et al. prepared Zr-PDC-20 to remove Glyphosate (Gly) from water. Zr-PDC-20 exhibited a high adsorption capacity of 423 mg/g due to its mesoporous structure with pore size range of 2–5 nm. Additionally, Zr-OH adsorption sites through ligand deletions are involved in the adsorption mechanism. Glyphosate adsorption was well fitted by the Langmuir isotherm model[26].

MIL-101(Cr) underwent a modification process involving the incorporation of amino ($NH_2$–) and urea ($UR_2$–) functional groups, aimed at enhancing its capacity for glyphosate adsorption.The adsorption kinetics were well-represented by a pseudo-second-order rate equation, while adsorption isotherms were analyzed using the Langmuir and Freundlich models.The $NH_2$-MIL-101(Cr) exhibited the highest adsorption capacity of 64.25 mg/g at a pH of 3.0.The introduction of the amino group enhanced the adsorption capacity of MIL-101(Cr), while the urea-modified variant, $UR_2$-MIL-101(Cr), significantly reduced this capacity. This suggests that, despite the potential for electrostatic attraction from both groups, the increased steric hindrance in $UR_2$-MIL-101(Cr) limits the access of GP to deeper pores[27].

Cu-BTC@CA was prepared by incorporation of various ratios of Cu-BTC (20–60%) within the CA membrane to uptake of dimethoate from water.40% Cu-BTC@CA showed a higher adsorption capacity of 321.9 mg/g for dimethoate. The Langmuir isotherm and pseudo-second order kinetics model adequately described the adsorption of dimethoate onto the prepared membrane. The recycled Cu-BTC@CA membrane showed effective reusability in adsorption of dimethoate, reducing the amount of adsorbed dimethoate by 22.5% after 5 reusing cycles. Adsorption of dimethoate on membranes involved physical and minor chemical processes. Dimethoate was deposited in the pores of the CA membrane and Cu-BTC MOF (Figure 3). Chemical adsorption occurred through electrostatic interactions, hydrogen bonding, and coordination bonding[28].

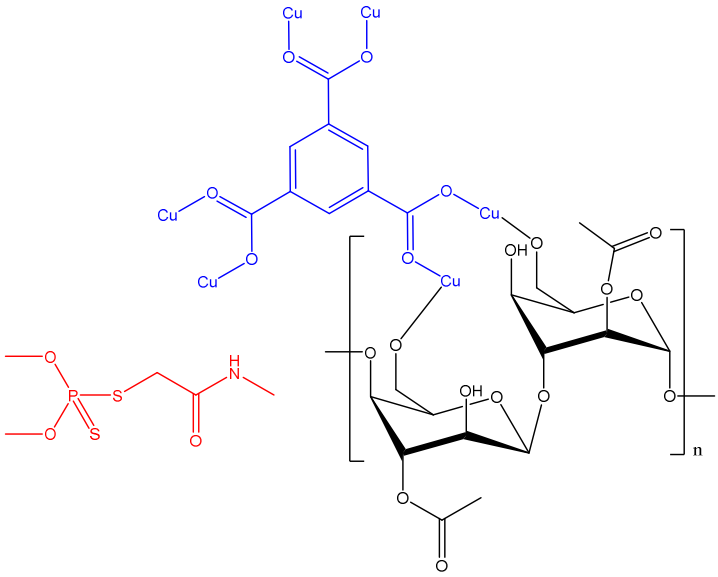


**Figure 3:** The interaction between dimethoate and the Cu-BTC@CA membrane.

Different amine ratio MOFs (Al-BDC, [Al-(BDC) $_{0.75}$(BDC-$NH_2$)$_{0.25}$], [Al-(BDC) $_{0.5}$(BDC-NH2)$_{0.5}$], [Al-(BDC) $_{0.25}$(BDC NH2)$_{0.75}$] and Al-BDC-$NH_2$) were successfully prepared to remove dimethoate from water. Al-(BDC) $_{0.5}$(BDC-$NH_2$)$_{0.5,}$ prepared by mixing equal molar amounts of terephthalic acid (BDC) with 2-aminoterephthalic acid (BDC-$NH_2$), a mixed organic linker, showed a higher adsorption capacity of 513.4 mg/ g for dimethoate. The adsorption process was investigated using experimental data and Monte Carlo simulation. The mechanism is based on hydrogen bonds and electrostatic interactions. The adsorption of dimethoate is enhanced by the amino group present on Al-BDCMOFs (Figure 4). The experimental results were more aligned with the pseudo first-order kinetic model, and the isothermal Langmuir model provided a more suitable approach for the description of equilibrium adsorption behaviour [29].

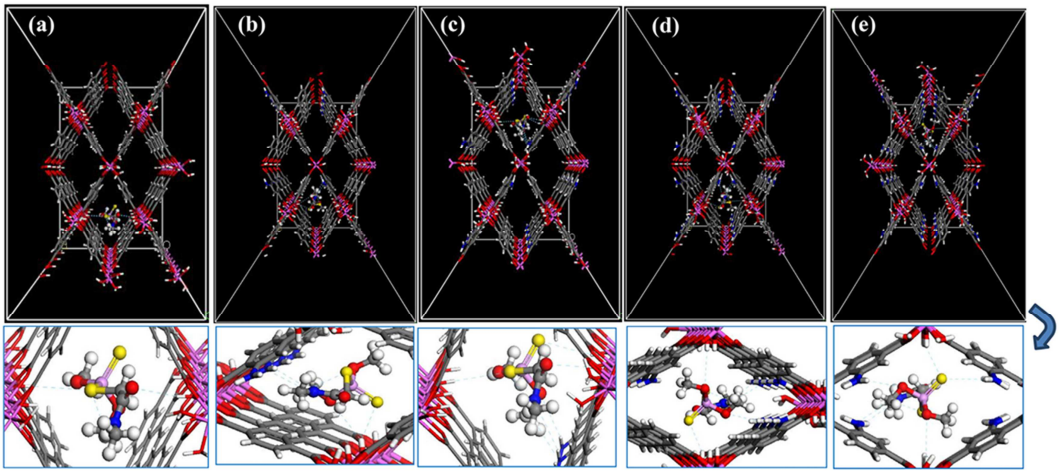


**Figure 4**: The lowest-energy structures of the adsorption of dimethoate onto the MOFs (100) surface (top view): (a) Al-BDC, (b) Al-(BDC) 0.75(BDC-$NH_2$)0.25, (c) Al-(BDC) 0.5(BDC-$NH_2$)0.5, (d) Al-(BDC) 0.25(BDC-$NH_2$)0.75, and (e) Al-BDC-$NH_2$, as obtained from the MC simulation.

The organophosphate insecticide diazinon (DZ) was extracted from water using a tin-metal organic framework (Sn-MOF) prepared by S.H. Alrefaee et al. The experiments showed that Sn-MOF is an effective adsorbent for extracting DZ from aqueous solutions. The results show that the maximum adsorption capacity of DZ onto Sn-MOF, with a value of 587.39 mg/g, requires a pH of 6. In particular, the pseudo-second-order model was used to thoroughly assess the effectiveness of DZ adsorption on Sn-MOF using kinetic models. Furthermore, the adsorption process was precisely fitted using the Langmuir isotherm model. The adsorption mechanism of diazinon was thought to happen chemically through π π interaction, H-bonding, and electrostatic interaction, or physically through pore filling (Figure 5) [30].

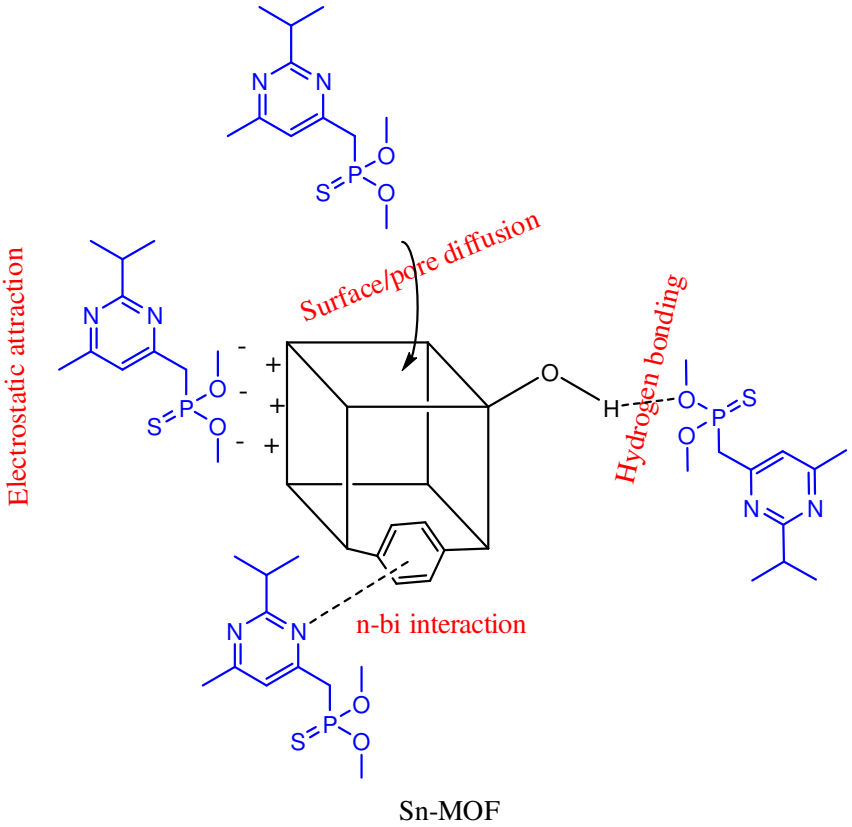


**Figure 5:** Adsorption mechanism of DZ onto Sn-MOF.

Fe-Cu-BTC, Co-Cu-BTC, and Mn-Cu-BTC are three copper-based organic frameworks that have been effectively synthesized to extract chlorpyrifos from aqueous medium. Chlorpyrifos had adsorption capacities of 379, 851, 683, and 762 mg/g over Fe-Cu-BTC, Co-Cu-BTC, and Mn-Cu-BTC, respectively. Fe-Cu-BTC had the highest chlorpyrifos adsorption capability, which may be attributed to the partial charge($Fe^{3+}$) on the metal in the MOF, increasing the number of active sites, improving the π-π interaction with chlorpyrifos' aromatic ring, or leading to the creation of an additional coordination bond (or strengthening the existing coordination bond).For the adsorption of chlorpyrifos, the appropriate kinetic model was pseudo-second-order. The Langmuir model adequately fitted the chlorpyrifos adsorption isotherm profile[31].

MIP-202 was fabricated with chitosan and alginate biopolymers to produce the composite MIP -202/CA beads. The Bio Zr-MOF beads were used to remove diazinon from wastewater. The so-synthesized composite exhibited the highest adsorption capacity, 17.77 mg/g. The Langmuir isotherm model described the diazinon adsorption process well and showed monolayer adsorption onto the produced MIP-202/CA beads. The higher adsorption capacity of MIP-202/CA composite beads was attributed mainly to the presence of excess hydroxide and amine groups on the beads' surface, resulting in strong attraction between the diazinon ions and the manufactured MIP-202/CA composite beads[32].

Yousefi et al. synthesized MOF-5 to remove diazinon from water. The highest adsorption capacity of diazinon onto MOF-5 was 44.4 mg/g. The adsorption of diazinon was well-fitted by the Langmuir isotherm model and the pseudo-first order kinetics model. The Garson equation was used as the basis for the sensitivity analysis, which evaluated the important critical variables in the ANN models. The weights derived from the superior neural network model and their partitioning are the basis for this analysis. The most effective variable was MOF-5 dosage; pH and mixing time had only a slight impact[33].

Chromium terephthalate metal organic framework (MIL-101(Cr)) was synthesized by the hydrothermal method to extract diazinon from wastewater. Response surface methodology (RSM) was used to optimize the adsorption process. The ideal parameters were pH 6.5, temperature 25°C, contact duration 64 minutes, and adsorbent dosage 0.74g/L, which resulted in a 96% elimination of diazinon. The maximum adsorption capacity of diazinon was determined to be 75.04 mg/g. The results showed that MIL-101(Cr) demonstrated a satisfactory removal percentage (71.32%) after five cycles, indicating the reusability of MIL-101(Cr). The adsorption of diazinon was best described by the pseudo second order kinetics model and the Langmuir isotherm model[34].

### 2.2. Removal of carbamate pesticides

Ca-Cu-BTC and Ca-Co-BTC were synthesized by the cold precipitation method developed by Abdelhamed et al. These novel Ca-based mixed metal-MOFs were used for the removal of carbofuran from wastewater. EPR analysis indicated that Ca-Cu-BTC displayed a doublet peak with broadening, and the g value was determined from the distinct hyperfine splitting peak to be 2.34. In contrast, Ca-Co-BTC showed pronounced broad peaks. Adsorption followed the second-order kinetic model and the Langmuir isotherm, suggesting a monolayer adsorption mechanism. For Ca-Co-BTC, the carbofuran adsorption capacity measured 627.26 mg/g, while for Ca-Cu-BTC, it was 736.31 mg/g. The high adsorption capacity of Ca-Cu-BTC is more than double that of the activated carbon and biochars. Adsorption mechanism of carbofuran proceeded via physical deposition in cavities and through chemical interactions, which primarily include coordination, hydrogen bonding, and π interactions(Figure 6)[35].

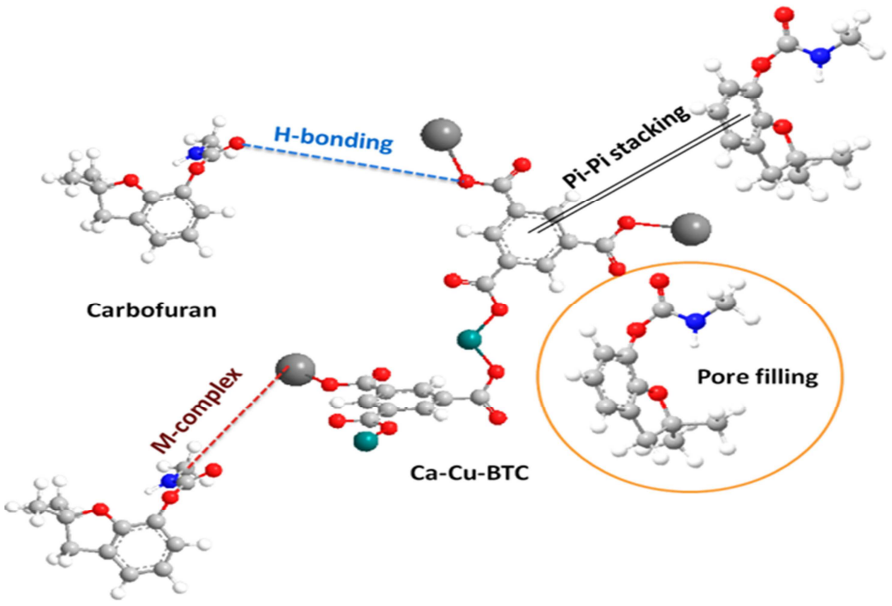


**Figure 6:** The adsorption mechanism of carbofuran onto Ca-M BTCs

Abdelhamed et al. used an aluminum-based metal-organic framework (MOF) for the uptake of carbofuran pesticide from wastewater. Complete characterization was done using XRD, SEM, $^{1}$HNMR, and IR for MIL-53-$NH_2$, and its modified forms, MIL-53-NH-ph, MIL 53-NH-ph-Fe, MIL-53-NH-ph-Zn, and MIL-53-NH-ph-Cu. The adsorption mechanisms involve a combination of stacking contact, coordination bonding, and hydrogen bond formation (Figure 7). The study found that carbofuran adsorption follows a pseudo-second-order kinetic model and fits well with the Langmuir isotherm model.MIL-53-$NH_2$, MIL-53-NH-Ph, MIL-53-NH-Ph-Fe, MIL 53-NH-Ph-Zn, and MIL-53-NH-Ph-Cu exhibited adsorption capacities of carbofuran pesticide, which were 367.8, 662.94, 717.6, and 978mg/g, respectively [1].

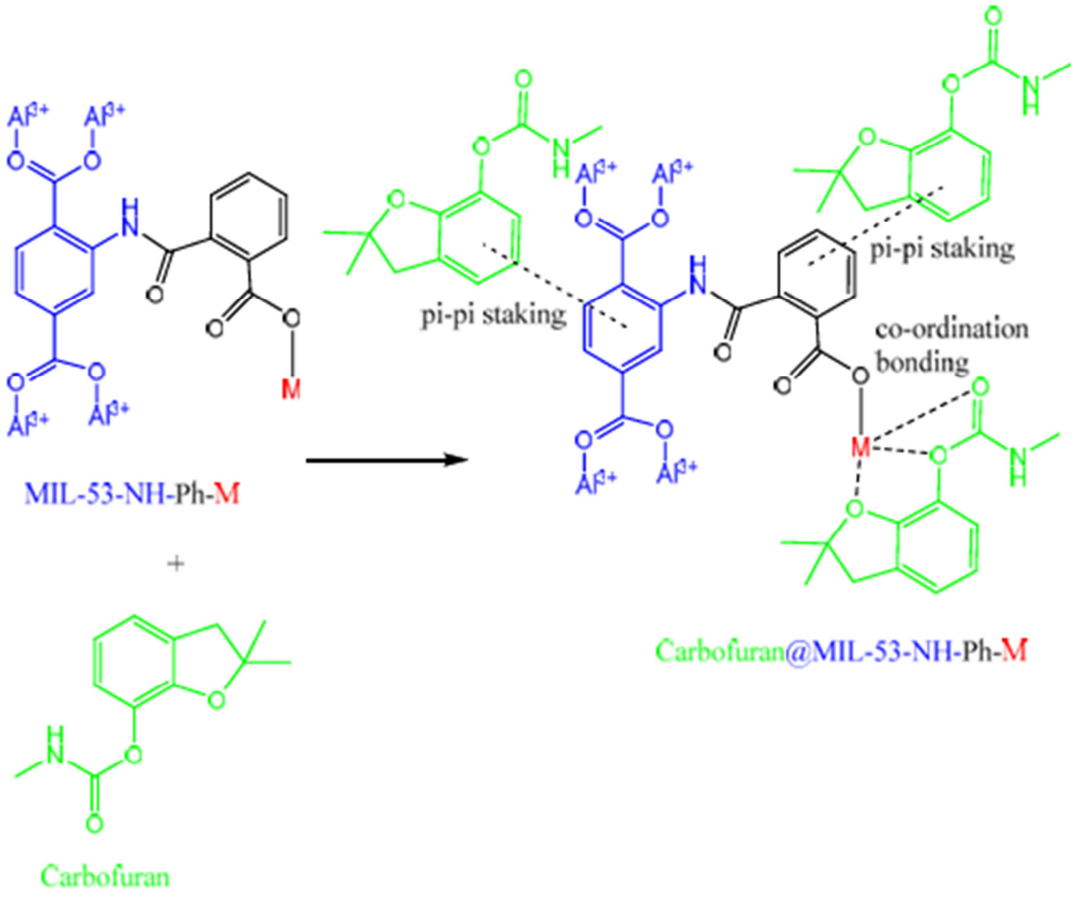


**Figure7:** Carbofuran adsorption mechanism onto the modified MIL-53-MOFs with transition metals.

Abdelhamed et al. prepared metal-organic frameworks based on aluminum to remove carbofuran from wastewater. These metal-organic frameworks include MIL-53-$NH_2$, MIL-53-AZA, MIL-53-AZA-La, and MIL-53-AZA-Ce. The adsorption process for carbofuran was best explained by pseudo-second-order kinetics and Langmuir isotherm models. The process currently involves a combination of π-π stacking interactions, coordination bonds, and the formation of hydrogen bonds (Figure 8). The highest capacities for eliminating carbofuran from water were measured as 367.87, 433.50, 610.23, and 635.05 mg/g for MIL-53-$NH_2$, MIL-53-AZA, MIL-53-AZA-La, and MIL-53-AZA-Ce, respectively [36].

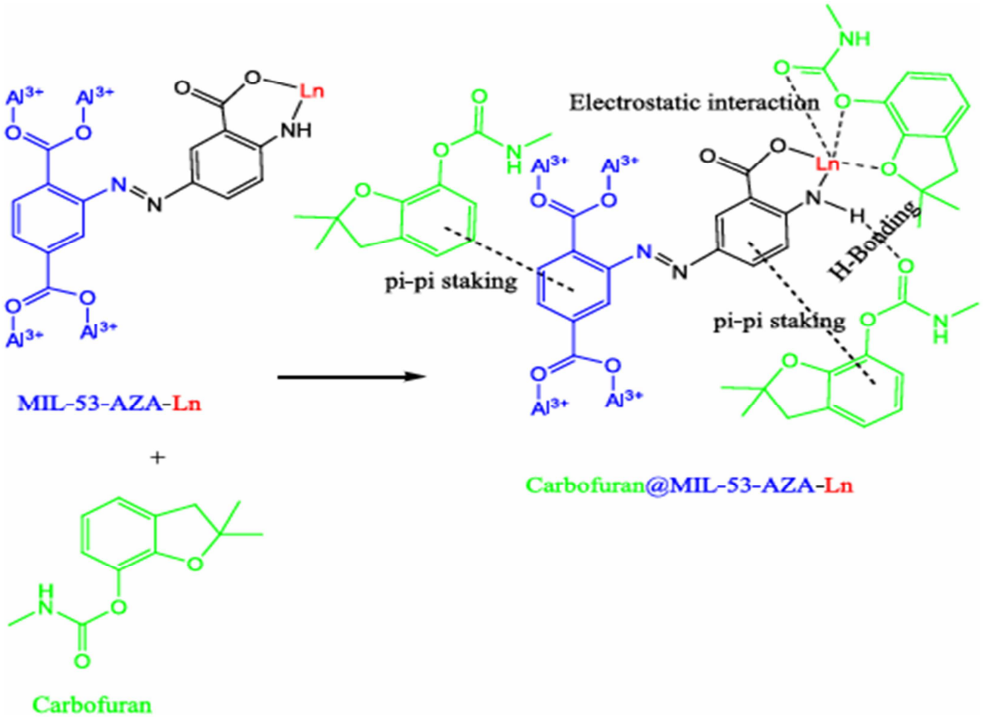


**Figure 8:** The mechanism of carofuran adsorption on the modified MIL-53-MOFs with lanthanide metal.

The effectiveness of Cu-BDC/ chitosan/alginic beads in eliminating carbaryl from contaminated water was demonstrated by Abdelhameed et al. The maximum adsorption capacity was determined to be 225.51 mg/g. Carbaryl adsorption was shown to follow the Langmuir isotherm model and to exhibit monolayer adsorption on Cu-BDC/chitosan/alginic granules. Efficient carbaryl adsorption on Cu-BDC, chitosan, and alginic beads can be achieved via chemical interaction via π-π stacking and H-bonding(Figure 9)[37].

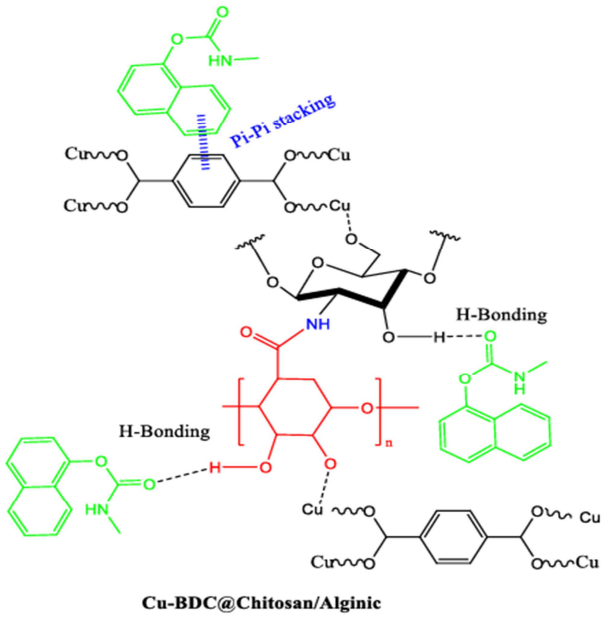


**Figure 9:** Carbaryl adsorption mechanism onto alginic/chitosan/Cu-BDC beads.

K. Qian et al. used MIL-101 to synthesize novel surface–imprinted nanoparticles. The synthesized MIL@MIP showed enhanced kinetic adsorption rate, BET SSA, and thermal stability. High selective adsorption affinity and satisfactory high transfer mass rates for metolcarb were demonstrated by the synthesized MIL@MIP. The maximum adsorption capacity of metolcarb was 152.76 mg/g[38].

The synthesis of Ca-MOF was accomplished by Z.A. Al-Ahmed through the utilization of solvothermal and microwave methodologies, yielding Ca-MOF-S and Ca-MOF-M, which exhibit sheaf and sheet structures, respectively. Ca-MOF with various morphologies has been used to study the removal of carbaryl and methomyl as carbamate insecticides from aqueous medium. Kinetic and isothermal studies showed that carbaryl had better adsorption than methomyl. Ca-MOF-M exhibited the highest adsorption capability, with maximum removal capacities of 500.36 mg/g for methomyl and 732.13 mg/g for carbaryl. Reusing Ca-MOF-M decreased the removal rate by 11% for carbaryl and 20% for methomyl, but it showed good reusability. The adsorption of carbaryl and methomyl on Ca-MOF-M and Ca-MOF-S surfaces involves intricate chemical mechanisms. These include hydrogen bonding, π-π interactions, electrostatic attractions, and strong van der Waals forces (Figure 10). The primary mechanism is π-π stacking due to the presence of pi systems in both carbaryl and Ca-MOF compounds, which facilitates the connection between aromatic rings, allowing for effective uptake of carbaryl from water [39].

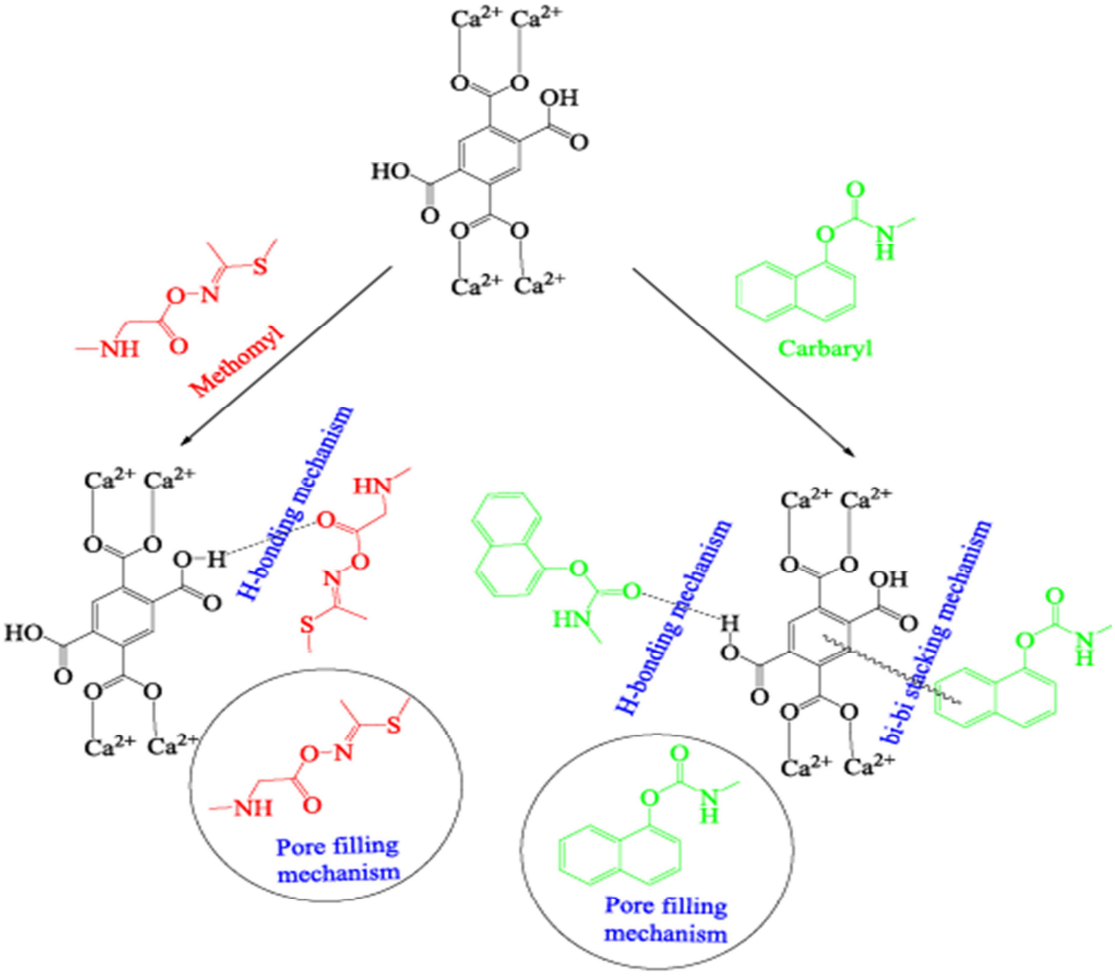


**Figure 10:** Mechanism of methomyl and carbaryl adsorption onto free carboxylic group functionalized Ca-MOFs.

### 2.3. Removal of herbicides

Cr-benzenedicarboxylate (MIL-53) has been investigated to adsorb 2,4-dichlorophenoxyaceticacid (2,4-D) from contaminated water.MIL-53has a substantially higher adsorption capacity than activated carbon or zeolite (USY) and a very quick absorption in one hour. The 2,4-D was removed using MIL-53 (Cr) with an adsorption capacity of 556 mg/g. The electrostatic interaction based on the MIL-53 zeta potential could explain the adsorption mechanism (Figure 11) [40].

\\

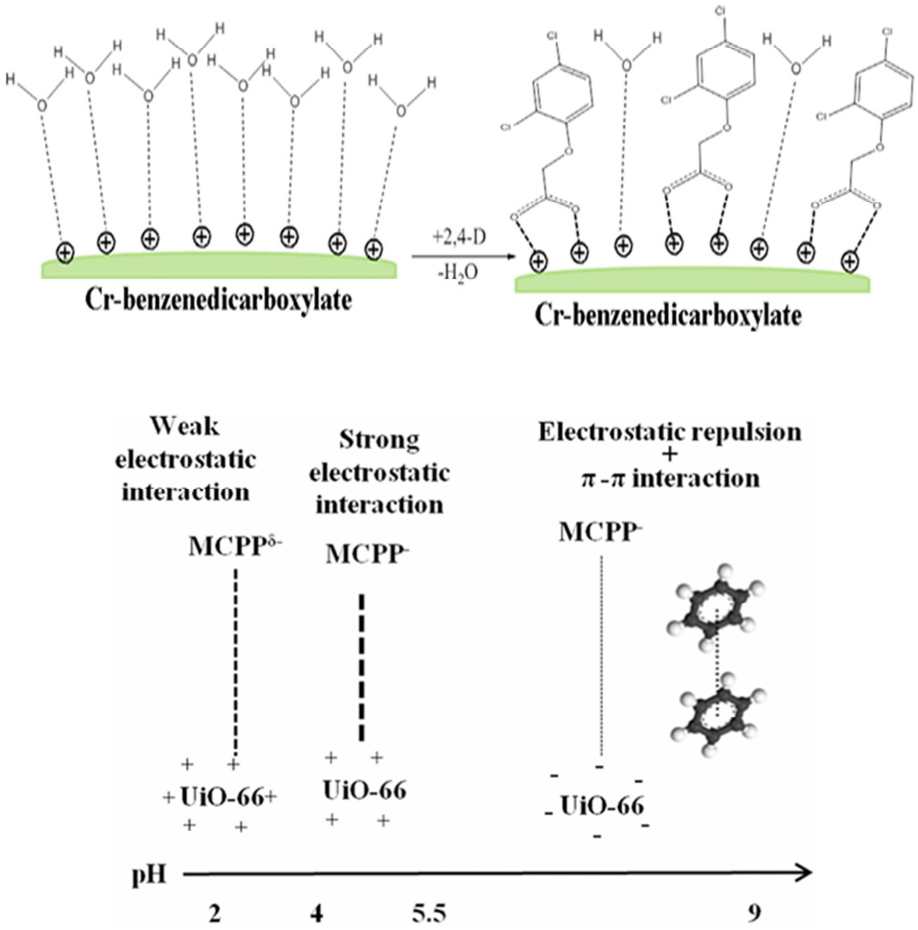


**Figure 11:** Mechanism for 2,4-D adsorption over MIL-53.

Zr-benzenedicarboxylate (UiO-66) was prepared by Y.S. Seo et al. to extract methylchlorophenoxypropionic acid (MCPP) from water. UiO-66 has a much higher adsorption rate than that of activated carbon. Additionally, UiO-66 has a higher adsorption capacity than activated carbon, particularly at low MCPP concentrations (7 points 5 times at 1 ppm of MCPP). The maximum adsorption capacity of MCPP onto UiO-66 was 370 mg/g. The adsorption process was explained by π-π interaction forces (at higher pH) and electrostatic bonding (at lower pH levels) [41].

E. Abdelillah Ali Elhussein et al. prepared $CeO_2$ nanofibers by calcination of Ce-BTC nanoparticles in an air furnace at 650°C for 3 h. The obtained $CeO_2$ nanofibers were used to remove 2,4-dichlorophenoxyacetic acid (2,4-D) from wastewater. It was determined through experimental studies that the ideal contact time was 100 minutes, and the ideal adsorbent concentration was 2.5 mg. The highest adsorption capacity was measured at 95–78 mg/g at 308 K. The adsorption of 2,4-D over $CeO_2$ nanofibers was considered to occur through boundary layer diffusion and intra-particle diffusion. The absorption of 2,4-D onto $CeO_2$ nanofibers was proposed to occur primarily through boundary layer diffusion and diffusion within the particle, respectively[42].

MIL-100(Fe) was demonstrated to be a powerful adsorbent for the adsorptive removal of the hazardous 2,4-D herbicide from aqueous solutions. The equilibrium data could be efficiently described by the pseudo-second-order kinetic equation and the Sips isotherm model, with a monolayer adsorption capacity for 2,4-D of 858.11 mg/g. The strong effects of ionic strength and solution pH on the adsorptive uptake indicated that the electrostatic attraction between the positively charged MIL-100(Fe) and the deprotonated 2,4-D was the dominant interaction (Figure 12) [43].

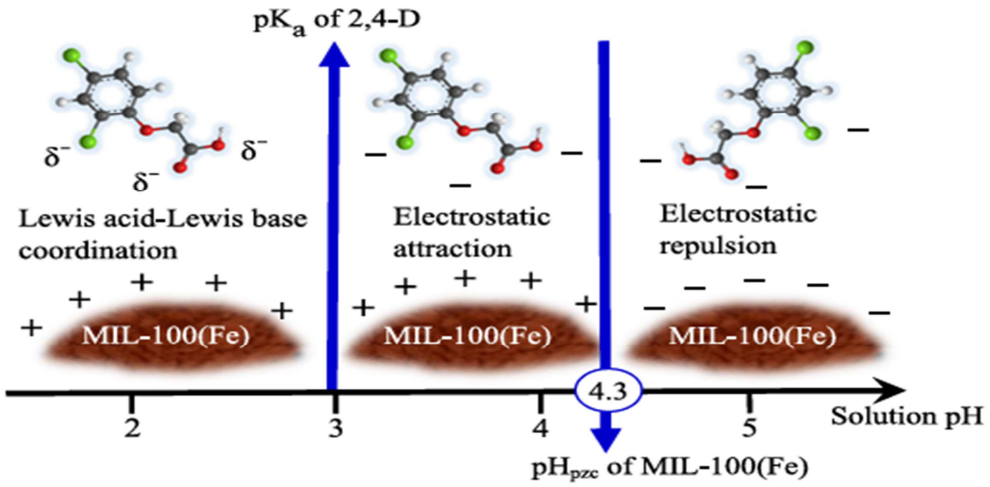


**Figure 12:** The adsorption mechanism of 2,4-D onto MIL-100(Fe)

Alsuhaibani et al. prepared Th-MOF to extract 2,4-dichlorophenylacetic (2,4-D) from aqueous solutions. The maximum 2,4-D adsorption onto Th-MOF was found to be 358.3 mg/g at a pH of 4. The Langmuir isotherm model fitted well to the adsorption process and consistently highlighted a chemisorption process. The mechanism of adsorption of 2,4-D over Th-MOF proceeded via Strong van der Waals force, pore filling, electrostatic interactions, π-π interactions, and hydrogen bonding (Figure 13). The synthetic Th-MOF adsorbent demonstrated remarkable cyclability and flexibility, effectively enduring up to six cycles of adsorption and desorption [44].

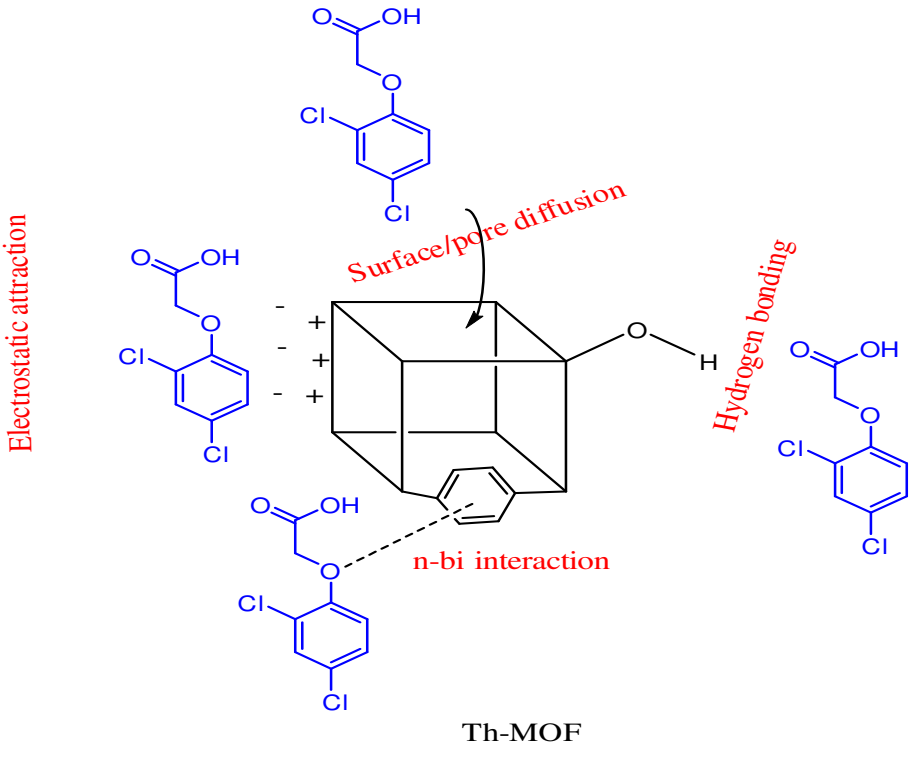


**Figure 13:** Mechanism of adsorption of 2,4-D over Th-MOF.

O. Alaysuy et al. prepared La/Zn-MOF to eliminate 2,4-dichlorophenylacetic acid (2,4-D) from wastewater. The maximum 2,4-D adsorption capacity on La/Zn-MOF, 307.5 mg/g, was attained at a pH of 6. The kinetic analysis revealed that the second-order model yielded better results than other kinetic models. Moreover, the diffusional model provided an accurate prediction of the changes in concentration over time. Numerous mechanisms, including π-π interaction, pore filling, H-bonding, and electrostatic contact, were proposed to explain the interaction between La/Zn-MOF and 2,4-D[45].

MIL-53(Al) was used to remove dicamba (3,6-dichloro-2-methoxy benzoic acid) and 4-chloro-2-methylphenoxyacetic acid (MCPA) from wastewater. MIL-53(Al) exhibited adsorption capacities of 228.5 and 231.9 mg/g for dicamba and MCPA, respectively. The adsorption process was best described by the Freundlich isotherm and the pseudo-second-order kinetics model. The experimental adsorption capacities of dicamba and MCPA were predicted using the RSM and ANN models. When compared to RSM, the projected values from the ANN model are more in line with the experimental results. The ANN model has higher determination coefficients and minimal error response compared to RSM for dicamba and MCPA, as it can generalize the nonlinear relationship between the actual and expected results and mimics the human brain.MIL-53(Al)demonstrated a noteworthy removal efficacy of 90%after five cycles of adsorption and desorption[46].

B. Liu et al. prepared FZM-4 by the hydrothermal method for the efficient uptake of 2,4-Dichlorophenoxyacetic acid (2, 4-D) from aqueous media. The so- prepared Fe–Zr-based metal- organic framework had a high surface area of 1003 $m^3/g$ with a lot of functional groups and a distinct surface charge. The highest adsorption capacity of FZM-4 for 2,4-D was measured at 357.14 mg per gram. The 2,4-D adsorption isotherms and kinetics on the FZM-4 follow the pseudo-second-order kinetic model and the Langmuir isothermal model, respectively. A concise description of the adsorption mechanism would be the combination of electrostatic interaction and hydrogen bonding, where π-π conjugation improved the FZM-4 adsorption effect on 2, 4-D(Figure 14)[47].

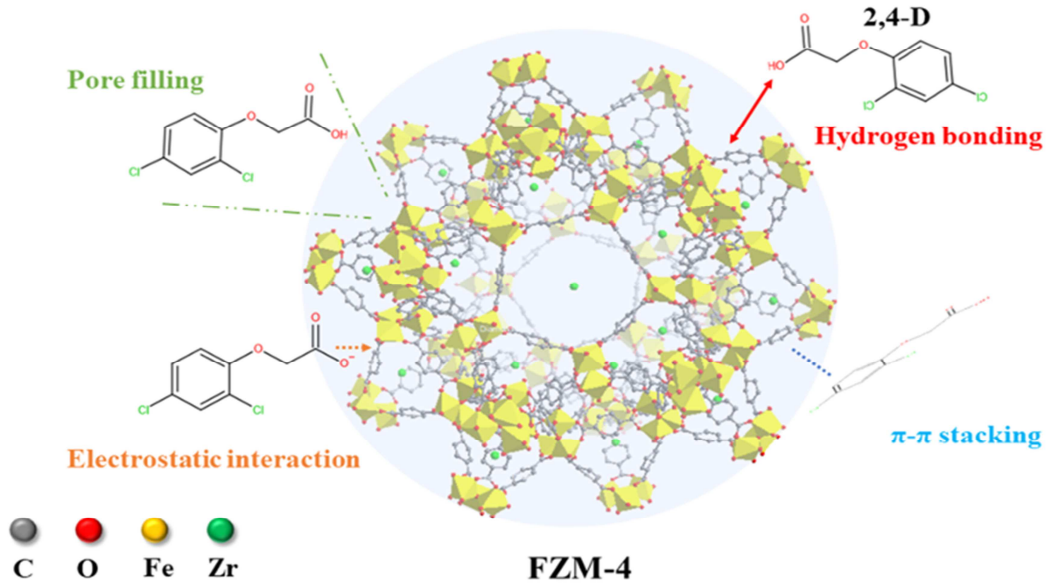


**Figure 14:** Mechanism of Adsorption of 2,4-D over FZM-4.

MIL-101(Cr)-$NH_2$ and UiO-66-$NH_2$ were synthesized using one-pot solvothermal reactionsto remove 2,4-dichlorophenoxyacetic acid (2,4-D) from aqueous media. The superior adsorption of 2,4-D on MIL-101(Cr)-$NH_2$ is due to its mesoporous structure, high surface area, large pore apertures, and abundant Cr metal clusters. These features enhance intra-particle diffusion and provide strong binding sites. The primary binding forces involve electrostatic interactions between the dissociated 2,4-D anion, metal clusters, and aminated benzene rings in the MOF. The pseudo-second-order kinetic model represented the adsorption of 2,4-D onto MIL-101(Cr)-$NH_2$ more accurately than the pseudo-first-order model. Additionally, the Freundlich model was closely followed by the adsorption isotherms [48].

Magnetic ruthenium metal-organic framework (MRM) was successfully evaluated for the uptake of 2,4-dichlorophenylacetic (2,4- D) from aqueous media. The efficiency of 2,4-D adsorption on MRM was investigated in detail using pseudo-second order kinetic models. Additionally, the Langmuir isotherm model accurately predicted the adsorption process. The results showed that the maximum 2,4-D adsorption capacity onto MRM is 293.93 mg/g at a pH of 4. The synthetically produced

MRM adsorbent may undergo up to five cycles of adsorption and desorption, demonstrating remarkable yield ability and reversibility. Adsorption mechanism of 2,4- D over MRM was described by π-π interactions, hydrogen bonding, electrostatic attraction, and pore filling (Figure 15) [49].

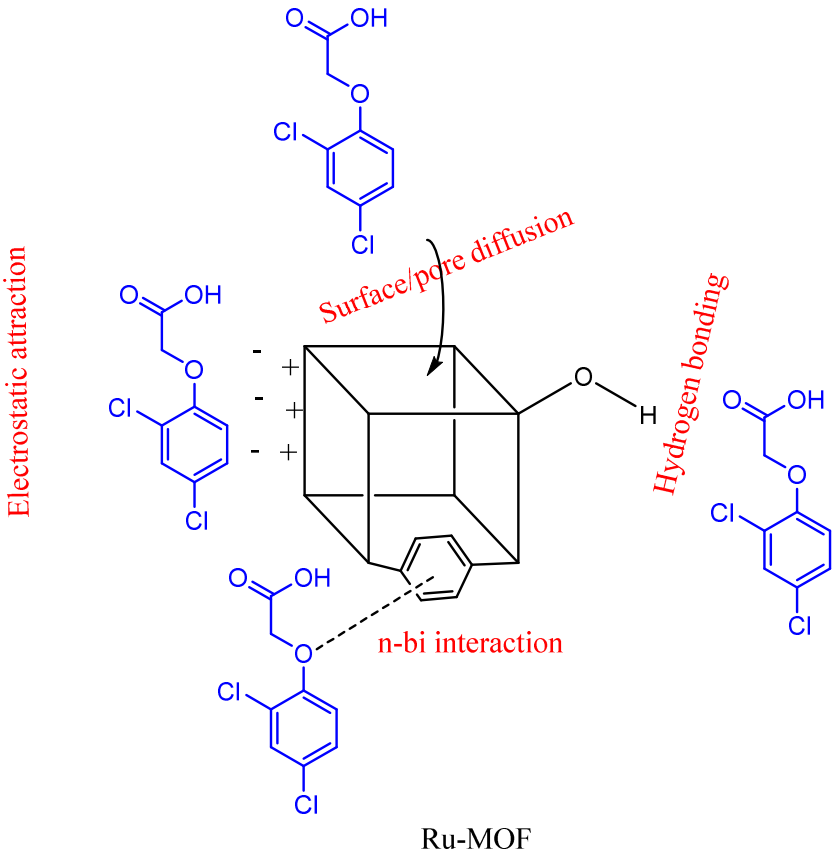


**Figure 15:** Interaction mechanism between MRM and 2,4-D.

Isiyaka et al. used MIL-101(Cr) to remove dicamba (3,6-dichloro-2-methoxy benzoic acid) from wastewater.MIL-101(Cr) had a high adsorption capacity (237.384 mg/g) and a high removal efficacy (99.432%) because of its quick equilibration (around 25 minutes) and huge surface area (1439 m2/g). The electrostatic interaction between the positively charged adsorbent surface and the negatively charged molecule was responsible for the high adsorption capacity. Adsorption capacity is influenced by the adsorbent dose and contact time, with 20 mg being the optimal dose for effective removal. MIL 101(Cr) demonstrated high reusability for dicamba removal in aqueous medium after three cycles, maintaining over 90% efficiency even after six cycles[50].

B. Huang et al. successfully prepared MOF-808 by the solvothermal method to remove 2,4-dichlorophenoxyacetic acid (2,4-D) and 2- methyl-4-chlorophenoxyacetic acid (MCPA) from aqueous media. MOF-808 had a specific surface area of 2,155 m²/g and demonstrated high adsorption capacities of 793 mg/g for 2,4-D and 775 mg/g for MCPA. The ideal pH values were 4.0 for MCPA and 3.0 for 2,4-D.The adsorption capacities of MOF-808 were shown to decrease slightly after five cycles, yet remained above 480 mg/g for 2,4-D and 479 mg/g for MCPA. The removal rates were 95. 9% and 95. 8%, indicating excellent reusability for MOF-808.FT-IR and XPS analyses revealed that the adsorption mechanisms involved electrostatic interactions, π-π interactions, hydrogen bonding, and complexation (Figure 16). The adsorption kinetics data indicated that the pseudo-second-order model provided a better fit than the pseudo-first-order model, suggesting chemisorption was the main mechanism in the adsorption process[51].

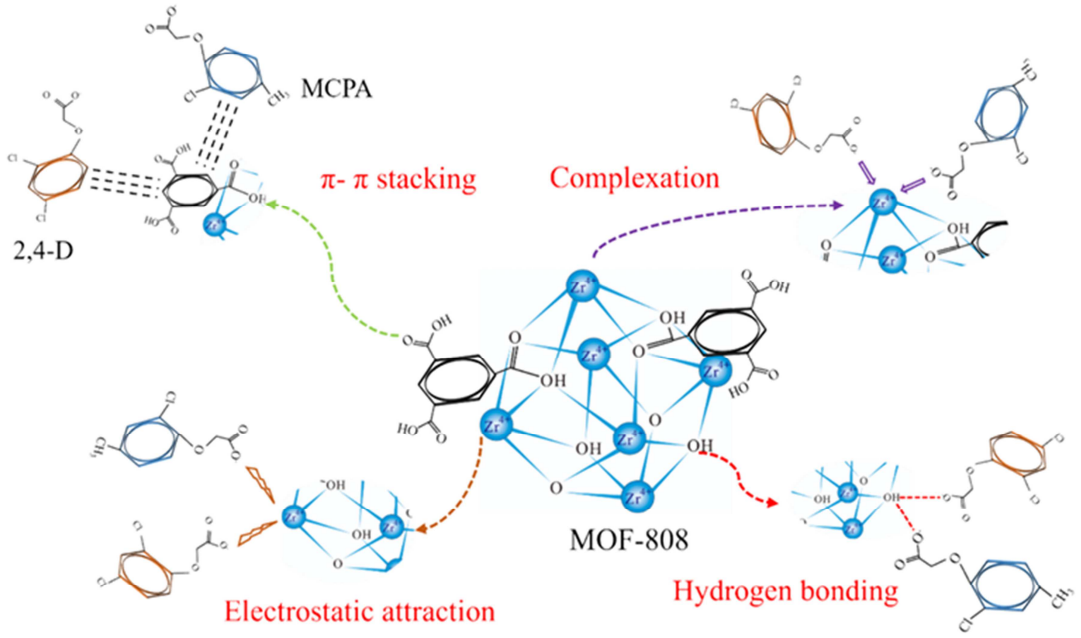


**Figure 16:** The likely mechanistic configuration of the PFOS molecules adsorbed on the MOF-808 surface.

UiO-66-$NH_2$ has been established to remove 2,4-Dichlorophenoxyacetic acid (2,4-D) from wastewater. UiO-66-$NH_2$ had a distinct adsorption capacity for 2,4-D, which was 215.5 mg/g. The high adsorption capacity of UiO-66-$NH_2$ was attributed to electrostatic, hydrogen bonding, and π–π interactions between MOFs and 2,4-D molecules. The greatest uptake of 2,4-D was noted at pH 7, where the zeta potentials (ζ) of UiO-66-$NH_2$ are mainly positive at 38.5 but negative for 2,4-D at -0.992[52].
H. Zhang et al. prepared Ce-MOF@PAN composite with antibacterial properties for the removal of 2,4-dichlorophenoxyacetic acid (2,4-D) from aqueous medium. The so-synthesized composite showed a maximum adsorption capacity of 200.80 mg/g. the high adsorption of 2,4-D was attributed to the high specific surface area and pore size of the composite fibrous membrane. Additionally, the adsorption mechanism includes hydrogen bonding, π π stacking, and electrostatic interaction[53].

Isil Akpinar prepared NU-1000(Zr) to remove atrazine from contaminated water. The adsorption capacity of atrazine over NU-1000(Zr) was 36 mg/g. Atrazine adsorption fits well with the Langmuir isotherm model[54].
UiO-67(Zr) was prepared by Isil Akpinar to remove atrazine from aqueous solution. The maximum adsorption capacity was determined to be 4.09 mg/g. The pseudo-second-order kinetic model fitted the atrazine adsorption[55].
Adsorptive removal of the agricultural pesticide atrazine from water was investigated using ZIF-8 and UiO-67. It was found that the adsorption capacity of atrazine over ZIF-8 and UiO-67 was 9.95 mg/g and 29 mg /g, respectively.ZIF-8 took more than 40 minutes to remove the same amount of atrazine from water, but UiO-67 removed 98% of it in just two minutes. UiO-67 showed lost less than 10% of its initial adsorption capacity at the conclusion of the third adsorption cycle. This outcome demonstrates that atrazine can be removed using UiO-67 multiple times. Atrazine adsorption in UiO-67 is best fitted by the Freundlich model, but ZIF-8 is best fitted by the Langmuir-Freundlich model [55].
Under optimized experimental conditions, $Cu_3(BTC)_2$ was electrochemically synthesized to uptake atrazine (ATZ) from wastewater. $Cu_3(BTC)_2$ had a high adsorption capacity of 484 mg/g for ATZ. The efficient uptake of $Cu_3(BTC)_2$ towards the toxic ATZ was shown in the presence of sunlight. The adsorption process has been approached from a variety of mechanistic perspectives, including hydrogen bonding, electrostatic interaction, framework metal influence, hydrophobic, π π and acid - base interaction [56].

Advanced oxidation techniques based on persulfate were combined with molecularly imprinted metal-organic frameworks (MMOFs) to effectively remove atrazine from wastewater. At pH 6, the MMOFs exhibited maximum adsorption capacities for atrazine, measuring 21.60 mg/g. Power pH values led to weak interactions due to increased $H^+$, whereas higher pH values resulted in an excess of $OH^-$ that damaged carboxyl groups, consequently decreasing the adsorption capacity of the adsorbents. The adsorption mechanism was established through hydrogen bonds, π-π stacking, and electrostatic forces. The adsorption mechanism involves hydrogen bonds, π-π stacking, and electrostatic forces, with atrazine's high electron affinity facilitating recognition. The copolymer fills MIL100 (Fe) channels, facilitating optimal binding via van der Waals forces. The

catalytic degradation of persulfate involves the formation of free radicals, which are confirmed through EPR, reducing the distance for diffusion between the radicals and atrazine. The MMOFs exhibited remarkable regeneration capability, maintaining a removal efficiency exceeding 72% after five cycles[57].

MIL-53(Al) was synthesized by the hydrothermal method to remove metolachlor (MET) from wastewater. MET exhibited high adsorption capacity of 241.617 mg/g over the synthesized MOF because of the MOF's large surface area (1104 $m^2/g$).Pseudo-second-order kinetics and Langmuir isothermal models were the best to describe the adsorption of MET from water.The MOF had a notable removal effectiveness of 92% after five cycles of adsorption and desorption, indicating the reusability of the adsorbent. The adsorption mechanism of MET over MIL-53(Al) demonstrated the existence of electrostatic interaction, hydrogen bonding, and π - π interaction between the MOF and MET[58].

B. Wang et al successfully prepared Cr-MIL-101 and Cr-MIL-101-BTP to remove acetochlor (ACT) from water. The adsorption capacity of ACT on Cr-MIL 101-BTP was greater than that of Cr-MIL-101.Cr-MIL-101-BTP exhibited maximum adsorption capacity of 312.5 mg/gf or ACT. The adsorption kinetics is efficiently described by the pseudo-second-order rate equation. The adsorption isotherm was better fitted by the Langmuir model than by the Freundlich model. The adsorption mechanism involved hydrogen bond and π-π stacking interactions[59].

### 2.4. Removal of neonicotinoid pesticides

MIL-101(Fe) and $NH_2$-MIL-101(Fe) were synthesized to eliminate acetamiprid (ATP) insecticide from aqueous solution. The highest ATP adsorption capacities on MIL 101(Fe) and $NH_2$-MIL-101(Fe) were 57.6 and 70.5, respectively. It was found that the ideal contact time for the ATP pesticide was 10 minutes. The adsorption process fits well with the Langmuir isotherm model and the adsorption kinetics are reasonably well described by the pseudo-2nd order model. Acetamiprid is removed by MIL-101(Fe) and NH2-MIL-101(Fe) primarily through electrostatic interactions. Inner sphere coordination, hydrogen bonding, and π-π stacking are also considered in the adsorption mechanism [60].

Isoreticularthioether-based MOFs derived from amino acids L-methionine and S-methyl-L cysteine were prepared to remove neonicotinoid insecticides (thiamethoxam, clothianidin, imidacloprid, acetamiprid, and thiacloprid) from wastewater. MTV-MOF-5, containing both amino acids in equal amounts, demonstrated exceptional higher adsorption capacities of 447,379,402,445, and 499 mg/g for thiamethoxam, clothianidin, imidacloprid, acetamiprid, and thiacloprid, respectively. The strong performance of 5 in capturing some NEO can be explained by X-ray crystallography. Interactions in acetamiprid@5 and thiacloprid@5, particularly related to sulfur ligands, play a significant role due to their spread in the nano confined space provided by 5. Both intra- and intermolecular interactions involving sulfur σ orbitals affect chemical reactivity, influencing kinetic, regiochemical, and stereochemical results. Electron-deficient bivalent sulfur atoms exhibit positive electrostatic areas for interacting with electron donors [61].

S. Singh, S. Kaushal, J. Kaur et al synthesized CaFu MOF for the efficient removal of imidacloprid from wastewater. The so-prepared MOF at pH 6.5 showed the highest adsorption of 467.23 mg/g for imidacloprid. The equilibrium adsorption of imidacloprid was described using Temkin, Freundlich, and Langmuir isotherms. The results obtained confirmed that the imidacloprid adsorption process correlates well with the Langmuir isotherm. The kinetic data were included in both pseudo-first-order and pseudo-second-order models, with the former being the more appropriate for imidacloprid adsorption on CaFu adsorbent. The adsorption mechanism was explained by non-covalent interactions Cl……H-O as well as coordination bonding between Ca ions and oxygen atoms of $NO_2$ group[62].

### 2.5. Removal of benzene-phenol derivatives

MIL-68(Al) and CAU-1 were applied for the removal of nitrobenzene (NB) from wastewater. Both aluminum-based MOFs demonstrated remarkably high NB adsorption capabilities from water. The highest adsorption capacities of NB onto MIL-68(Al) and CAU-1 were 1188.33 mg/g and 1171.65 mg/g, respectively. The Langmuir and pseudo-second-order models are appropriate for representing the NB adsorption processes in CAU-1 and MIL-68(Al). The adsorption process of NB may be significantly influenced by the $\mu_2$-OH in Al–O–Al units of Al-MOFs [63].

Cu-BTC@C-PAN was successfully prepared to remove 4-chlorophenol (4-CP) and 4-chlorophenol (4-CP) from water. The newly developed beads exhibited exceptionally high adsorption capabilities for 4-CP and 4-NP, measuring 277.02 and 324.74 mg/g, respectively. The adsorption mechanism demonstrated that phenols can be adsorbed onto prepared MOF beads through physical and chemical adsorption. Physical adsorption occurs within the pores of the beads, while chemical adsorption occurs through coordination or hydrogen bonds as well as π – π interaction. The higher adsorption of 4-NP with Cu-BTC@C-PAN beads is due to the higher reactive sites in both C-PAN and MOF Cu-BTC. The NH group of C-PAN can be protonated and then adsorbs 4-NP easily and faster through electrostatic attraction (Figure 17). The amide group in Cu-BTC@C-PAN beads also acts as a trap for 4-NP, showing strong affinity and transferring electrons to the nitro group in the large conjugated ring [64].

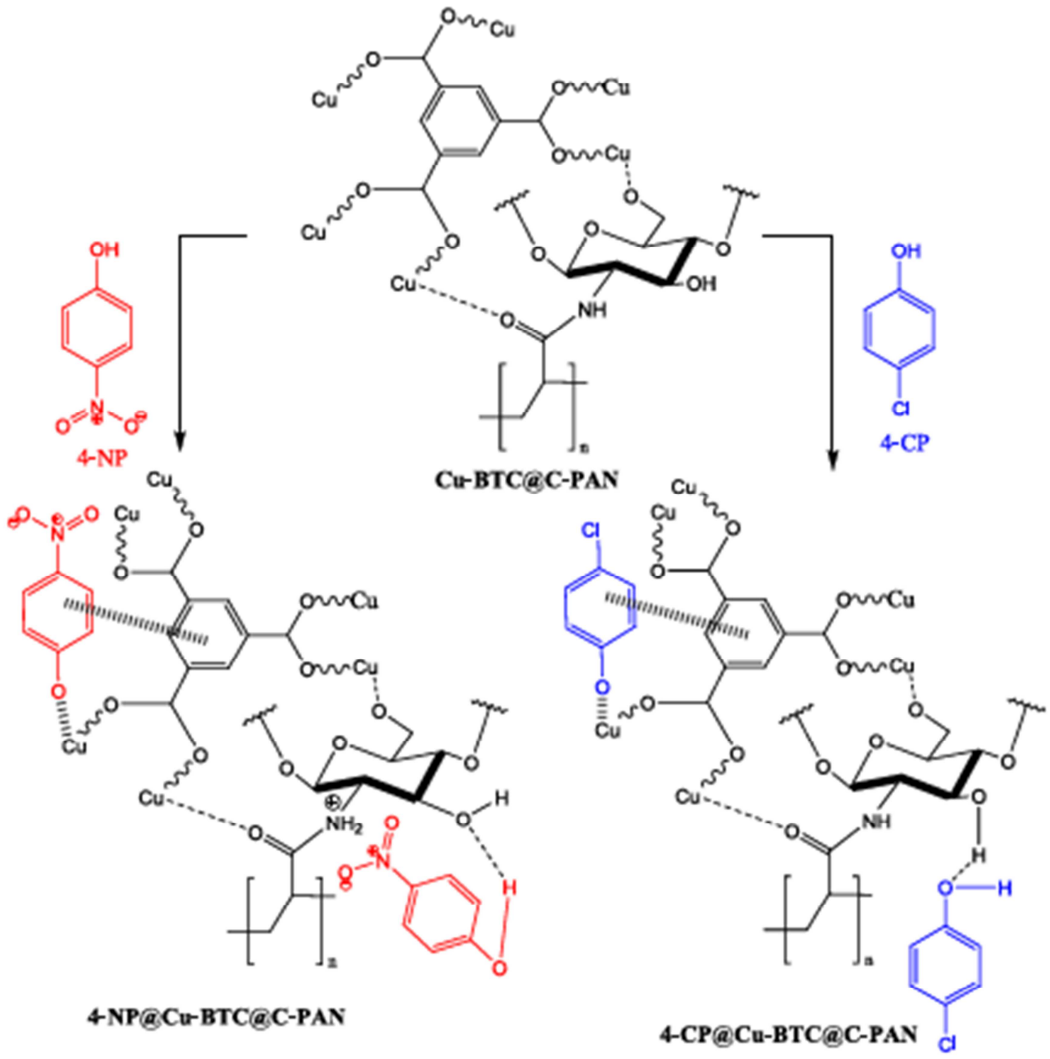


**Figure 17:** Adsorption mechanism of phenols onto Cu-BTC@C-PAN.

### 2.6. Removal of boron

ZIF-8 was prepared and tested to uptake boric acid from aqueous media.ZIF-8 exhibited a high boron adsorption capacity of 247.44 mg/g. The isotherms are well described by the Freundlich model, which also implies that chemisorption is crucial to the adsorption process. The adsorption mechanism revealed strong interactions between boric acid and Zn sites, with four $B(OH)_3$ molecules adsorbed at three distinct sites in a unit cell. ZIF-8 cannot be regenerated with water, but its boron adsorption capacity almost remains unchanged due to its large surface area and pore volume[65].

Cobalt-based ZIF-67 was synthesized to remove boron from water.ZIF-67 had a well-defined rhombic dodecahedron with a particle size of roughly 400−500 nm. With an optimum pH of 4, ZIF-67 demonstrated the highest absorption capacity of 579.80 mg/g. The mechanism of Boron adsorption over ZIF-67 was considered to proceed via π–π stacking interaction, electrostatic attraction and the coordination bonding between open metal ion sites in ZIF-67 and polymeric borate ions. The ZIF-67 adsorption capacity at the fifth regeneration cycle may still display 94.1% of its initial capacity[66].

### 2.7. Removal of pyrethroid pesticides

Detamethrin (DEL) was removed from wastewater using innovative lanthanum metal-organic frameworks (La-MOFs). The adsorption capacity of the La-MOF is 227.34 mg/g at pH values near 4, which is the pH at which adsorption is most effective. The pseudo-second-order model and the Langmuir adsorption isotherm model provided a good explanation of the DEL uptake process. The interactions between La-MOF and DEL were investigated (Figure 18). Surface pore diffusion, π–π interaction, electrostatic interaction, and hydrogen bonding all contribute to the adsorption process[67].

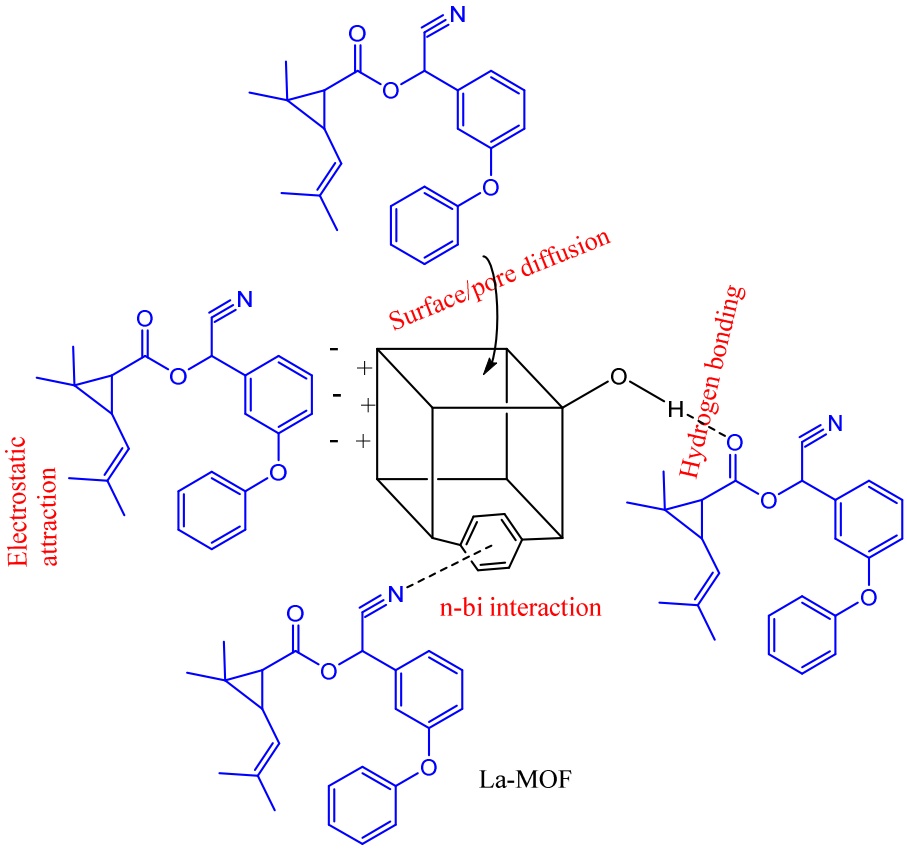


**Figure 18:** La-MOF and DEL interaction mechanism

A.T. Mogharbel et al. prepared Tb/Pd-MOF to remove the herbicide paraquat from water. The highest adsorption capacity of 574.8 mg/g was observed at a pH level of 8. The Langmuir adsorption isotherm model was found to be the most appropriate isotherm model for describing the adsorption process. The pseudo-second-order model was shown to be the best fit for the data by the kinetic analysis. Adsorption mechanism of paraquat herbicide was mainly attributed to electrostatic interactions between the paraquat and the MOF. Furthermore, the Van der Walls forces and π-π interactions and pore-filling are involved in the adsorption process[68].

Paraquat was effectively extracted from wastewater using Fe-BTC and ZIF-8. Both adsorbents demonstrate high specific surface areas (SBET) of 1765 m²/g for ZIF-8 and 1790 m²/g for Fe-BTC, leading to significant adsorption capacities of 713.65 mg/g and 1012.8 mg/g, respectively. Adsorption isotherms were best fitted by the Langmuir model, while ZIF-8 and Fe-BTC kinetic data were correctly predicted by pseudo-first-order and pseudo-second-order models.Paraquat is mostly adsorbed by ZIF-8 via electrostatic interactions, which are especially efficient at neutral pH. Fe-BTC performs chemisorption, which maximizes its adsorption in acidic environments because of improved ion-pair interactions. The Fe-BTC adsorbent has limited regeneration capabilities due to the strong chemical bonds formed with paraquat. In contrast, the ZIF-8 adsorbent showed better results, recovering 85% efficiency initially and retaining 74. 6% capacity after four cycles, proving its stability and reusability for water treatment[69].

MOF-74(Zn)-derived carbon (CDM-74) was synthesized by Bhadra et al. through the pyrolysis of Zn-based MOF-74 to remove N, N diethyl-3-methylbenzamide (DEET) insecticide and many other pollutants. The synthesized MOF showed a maximum adsorption capacity of 340 mg/g for DEET. Because DEET is neutral and has a low pH, electrostatic interactions—which are frequently used to explain organic/aromatic adsorption from water—have less of an impact on its structure. DEET adsorption over CDM-74 may be explained by H-bonding because of acidic groups, particularly carboxylic and phenolic groups. The H-donor atom of the carboxylic or phenol group can facilitate DEET adsorption via H-bonding with the O-atom and partly N-atom. The van der Waals interaction, pore filling, or the acidity of functional groups can all account for the

consistent drop in q12 h with pH. When assessing its recyclability for DEET adsorption, CDM-74 showed remarkable performance and competitiveness even after regeneration for up to four cycles[70].
MOF-808 was synthesized and characterized to remove Perfluorooctanesulfonate (PFOS) from wastewater. The novel MOF-808 had a large specific surface area (1610 $m^2/g$), a well-crystalline structure, and exceptional stability in an aqueous medium.MOF-808 was an exceptional adsorbent for removing PFOS from aqueous solution, according to the adsorption results, with a maximum adsorption capacity of 939 mg/g. PFOS adsorption onto MOF-808 is primarily mediated by the electrostatic interaction between the PFOS anion and the cationic central cluster ($[Zr_6O_4(OH)_4]_{12}^{+}$) of MOF-808(Figure 19)[71].

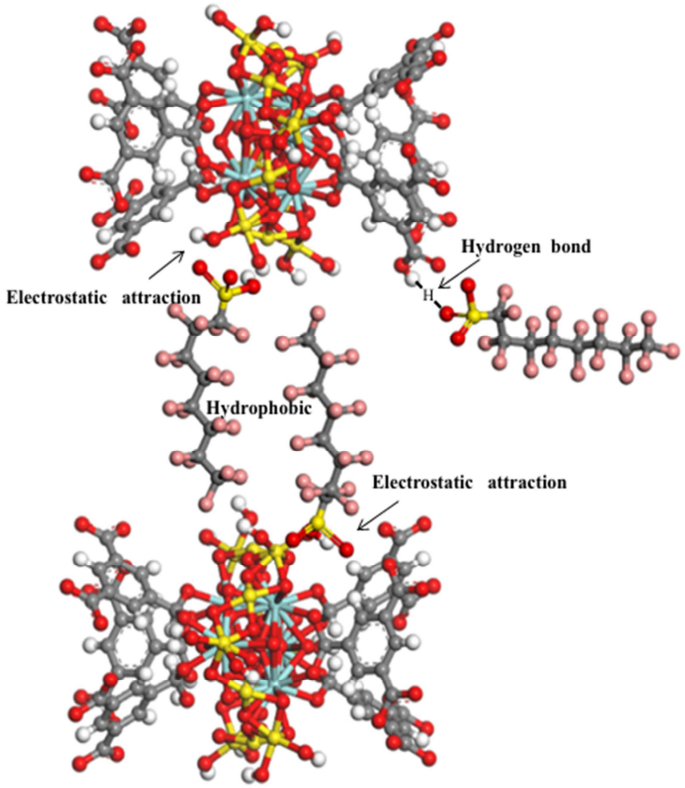


**Figure 19:** The probable molecular configuration of PFOS molecules adsorbed on the MOF-808 surface.

MOFs show varying pesticide adsorption capacities depending on their structure and the specific pesticide. Some MOFs, like MIL-53, have shown high adsorption capacities for certain pesticides, such as carbofuran (978 mg/g). Other MOFs, including ZIF-8 and ZIF-67, have demonstrated different adsorption capacities for various pesticides like prothiofos and ethion. The adsorption capacity is influenced by factors like the MOF's pore size, surface area, and specific interactions with the pesticide molecules. Table 1 shows the comparison of maximum adsorption uptake of pesticides on different MOF structures with previously published material. In summary, MOFs offer a promising platform for pesticide removal due to their tunable properties and high adsorption capacities. By carefully selecting the MOF structure, composition, and functional groups, it is possible to design MOFs that are highly effective at removing specific pesticides from contaminated water sources.

**Table 1:** Maximum adsorption uptake of pesticides on different MOFs structures

| MOFs name | Pesticide name | Adsorption capacity mg/g | References |
|---|---|---|---|
| Ca-Cu-BTC | Carbofuran | 736.31 | [10] |
| Ca-Co-BTC | | 627.26 | |
| MIL-53-NH-Ph-Cu | Carbofuran | 978.60 | [1] |
| MIL-53-NH-Ph-Zn MIL-53-NH-Ph-Fe MIL-53-NH-Ph | Carbofuran | 717.60<br>662.90<br>462.10 | |
| MIL-53-$NH_2$ | | 367.90 | |
| MIL-53-AZA-La | Carbofuran | 635.1 | [36] |
| MIL-53-AZA-Ce | | 610.2 | |
| MIL-53-AZA | | 433.5 | |
| MIL-53-NH2 | | 367.8 | |
| Cu–BTC@cotton | Ethion | 182 | [20] |
| Zr-MOF@Ox-cotton | Diazinon | 464.69 | [21] |
| | Chlorpyrifos | 389.69 | |
| Cu-BDC/chitosan/alginic beads | Carbaryl | 225.51 | [37] |
| MIL@MIP | Metolcarb | 152.67 | [38] |
| Sn-MOF | Diazinon | 587.395 | [30] |
| MIL-53 (Cr) | 2, 4-Dichlorophenoxyacetic acid | 556 | [40] |
| MIL-101(Fe) | Acetamiprid | 57.6 | [72] |
| $NH_2$-MIL-101(Fe) | | 70.5 | |
| Cu-BTC | $^{14}$C-Ethion | 122 | [73] |
| ZIF-8 (Zn) | Prothiofos | 366.7 | [23] |
| | Ethion | 279.3 | |
| ZIF-67(Co) | Prothiofos | 261.1 | |
| | Ethion | 210.8 | |
| UiO-66(Zr) | Methylchlorophenoxypropionic acid | 370 | [41] |
| NU-1000(Zr) | Glyphosate | 1516 | [25] |
| UiO-67(Zr) | | 1335 | |
| NU-1000(Zr) | Atrazine | 36 | [54] |
| UiO-67(Zr) | Atrazine | 4.09 | [55] |
| UiO-67(Zr) | Dichlorvos | 571.43 | [24] |
| | Metrifonate | 378.78 | |
| UiO-66(Zr) | Dichlorvos | 172.40 | |
| | Metrifonate | 90.94 | |
| Ce-BTC | 2,4-Dichlorophenoxyacetic acid | 95.78 | [42] |
| MIL-100 (Fe) | 2,4-Dichlorophenoxyacetic acid | 858.11 | [43] |
| ZIF-8(Zn) | Atrazine | 9.95 | [55] |
| UiO-67 (Zr) | | 29 | |
| MOF-808 | Perfluorooctanesulfonate | 939 | [71] |
| MIL-68(Al) | Nitrobenzene | 1188.3 | [74] |
| CAU-1 | | 1171.65 | |
| ZIF-8(Zn) | Boric acid(boron) | 247.44 | [65] |
| ZIF-67(Co) | Boric acid(boron) | 579.8 | [66] |
| Th-MOF | (2,4-D) | 358.3 | [44] |
| MOF-5 | Diazinon | 44.4 | [33] |
| MIP-202/CA beads | Diazinon | 17.77 | [32] |
| La/Zn-MOF | (2,4-D) | 307.5 | [45] |
| $Cu_3(BTC)_2$ | Atrazine | 484 | [56] |
| MIL-101(Cr)-$NH_2$ | 2,4-D | 348.5 | [48] |
| UiO-66-$NH_2$ | | 367.2 | |
| UiO-66-$NH_2$ | 2,4-D | 215.5 | [52] |
| FZM-4 | 2,4-D | 357.14 | [47] |
| Fe-Cu-BTC | Chlorpyrifos | 851 | [31] |
| Co–Cu-BTC | | 683 | |
| Mn-CuBTC | | 762 | |
| MIL-53(Al) | Metolachlor | 241.617 | [58] |
| La-MOF | Deltamethrin | 227.34 | [67] |

| | | | |
|---|---|---|---|
| MIL-53(Al) | Dicamba (3,6-dichloro-2-methoxy benzoic acid) | 228.5 | [46] |
| | MCPA (4chloro-2-methylphenoxyacetic | 231.9 | |
| Tb/PdMOF | Paraquat herbicide | 574.8 | [68] |
| MRM | 2,4-D | 293.93 | [49] |
| MIL-101(Cr) | Diazinon | 75.04 | [34] |
| Zr-PDC-20 | Glyphosate | 423 | [26] |
| Cu-BTC@C-PAN | 4-NP | 324.74 | [64] |
| | 4-CP | 277.02 | |
| Cu-BTC@CA | Dimethoate | 321.9 | [28] |
| MTV-MOF 5 | Thiamethoxam | 447 | [61] |
| | Clothianidin | 379 | |
| | Imidacloprid | 402 | |
| | Acetamiprid | 445 | |
| | Thiacloprid | 499 | |
| Amino-Al-MIL-53 | Dimethoate | 513.4 | [29] |
| MIL-101(Cr) | Dicamba | 237 | [75] |
| Ce-MOF@PAN | 2,4-D | 200.80 | [53] |
| Cr-MIL-101 | Acetochlor | 118.7 | [59] |
| Cr-MIL-101-BTP | | 312.5 | |
| CaFu MOF | Imidacloprid | 467.23 | [62] |
| CDM-74 | DEET | 340 | [70] |
| $NH_2$-MIL-101(Cr) | Glyphosate | 64.25 | [27] |
| Urea-MIL-101(Cr) | | 25 | |
| MOF-808 | 2,4-D | 793 | [51] |
| | MCPA | 775 | |
| Ca-MOF-S | Carbaryl | 366.64 | [39] |
| Ca-MOF-M | | 732.13 | |
| | Methomyl | 179.72 | |
| | | 500.35 | |
| Fe-BTC | Paraquat | 1012.8 | [76] |
| ZIF-8 | | 713.65 | |
| MMOF | Atrazine | 21.60 | [77] |

## 3. Conclusion

The applications of metal-organic frameworks (MOFs) in the pesticides sector included adsorption, delivery, and sensing. MOFs' advantages were high porosity, adjustable pore size, and the ability to interact with specific molecules. Thanks to their specific surface areas and high porosity, MOFs can interact with and capture pesticides, enabling their detection. Adsorption and removal of pesticides play a perfect role in MOFs' application due to their high surface area and high porosity. MOFs enable the efficient adsorption and removal of pesticides from water and other materials. To concentrate and remove pesticides, MOFs can be used as adsorbents.

The high porosity, large surface area, and adjustable pore size of MOFs make them promising materials for removing pesticides from water. The adsorption process, in which pesticides adhere to the surface and pores of the MOF structure, is the main removal mechanism. The adsorption process involves several interactions, such as coordination bonding, π-π stacking, electrostatic interactions, and hydrogen bonding. The factors behind the adsorption mechanism can be summarized as follows: i) Porous structure: MOFs feature a large surface area and a highly porous structure, providing pesticides with ample surface area for adsorption. ii) Interactions: The adsorption process is driven by multiple intermolecular forces, including hydrogen bonding, where the organic ligands or metal centers of the MOF interact with the pesticides capable of forming hydrogen bonds and π-π stacking: The π electrons of the MOF organic ligands interact with the aromatic structures present in the pesticides. Electrostatic interactions may arise if the surface of the pesticide or MOF is charged. Coordination bonding: The free metal centers present in some MOFs can coordinate with the pesticides to form a complex. Functional Use: The structure of MOFs can be altered to improve the interactions of specific pesticides. Advantages of pesticide removal using MOFs: high adsorption capacity: MOFs can adsorb large amounts of pesticides due to their large surface area and porous structure. Tunability: By modifying the structure of MOFs, the removal process can be optimized to target specific pesticides. Reusability: After pesticide adsorption, some MOFs can be recovered and reused, reducing material waste.

## 4. References

1. Nabil, M., et al., *Remarkable separation of carbofuran pesticide from aqueous solution using free metal ion variation on aluminum-based metal-organic framework.* Colloids and Interfaces, 2022. **6**(4): p. 73.
2. Abdel-Gawad, H., et al., *Distribution and degradation of 14C-ethyl prothiofos in a potato plant and the effect of processing*. Phosphorus, Sulfur, and Silicon and the Related Elements, 2008. **183**(11): p. 2734-2751.

3. Witczak, A., et al., *Residues of some organophosphorus pesticides on and in fruits and vegetables available in Poland, an assessment based on the European union regulations and health assessment for human populations.* Phosphorus, Sulfur, and Silicon and the Related Elements, 2018. **193**(11): p. 711-720.
4. Witczak, A., et al., *Tracking residual organochlorine pesticides (OCPs) in green, herbal, and black tea leaves and infusions of commercially available tea products marketed in Poland.* Food Additives & Contaminants: Part A, 2018. **35**(3): p. 479-486.
5. Ahmad, M.F., et al., *Pesticides impacts on human health and the environment with their mechanisms of action and possible countermeasures.* Heliyon, 2024.
6. Gamal, E.A., et al., *Ammonia removal from simulated fish farms by metal organic framework ingrained by egg shell and fish bones.* Scientific Reports, 2025. **15**(1): p. 1-19.
7. Emam, H.E., R.M. Abdelhameed, and H.B. Ahmed, *Metal Organic Framework (MOF)-Based Advanced Materials for Clean Environment*, in *Advanced Materials for a Sustainable Environment*. 2022, CRC Press. p. 159-188.
8. Emam, H.E., et al., *Selective separation of chlorophyll-a using recyclable hybrids based on Zn-MOF@ cellulosic fibers.* Scientific Reports, 2023. **13**(1): p. 15208.
9. Emam, H.E. and R.M. Abdelhameed, *Separation of anthocyanin from roselle extract by cationic nano-rode ZIF-8 constructed using removable template.* Journal of Molecular Structure, 2022. **1267**: p. 133607.
10. Emam, H.E., et al., *Synthesis, spectroscopic study and carbofuran adsorption of mixed metal (Co, Cu)@ Ca-BTC frameworks aimed at wastewater cleaning.* Journal of Industrial and Engineering Chemistry, 2024. **139**: p. 444-457.
11. M. Abdelhameed, R., et al., *Engineering ZIF-8 hybridization by extracted lignin with antibacterial property for uptake of methomyl residues from wastewater.* Separation Science and Technology, 2022. **57**(18): p. 3023-3034.
12. Abdelhameed, R.M., O.M. Darwesh, and M. El-Shahat, *Titanium-based metal-organic framework capsulated with magnetic nanoparticles: Antimicrobial and photocatalytic degradation of pesticides.* Microporous and Mesoporous Materials, 2023. **354**: p. 112543.
13. Abazari, R., et al., *Design and engineering of MOF/LDH hybrid nanocomposites and LDHs derived from MOF templates for electrochemical energy conversion/storage and environmental remediation: Mechanism and future perspectives.* Coordination Chemistry Reviews, 2025. **523**: p. 216256.
14. Li, J., et al., *Metal-organic frameworks as superior adsorbents for pesticide removal from water: The cutting-edge in characterization, tailoring, and application potentials.* Coordination Chemistry Reviews, 2023. **493**: p. 215303.
15. Bagheri, A.R., N. Aramesh, and M. Bilal, *New frontiers and prospects of metal-organic frameworks for removal, determination, and sensing of pesticides.* Environmental Research, 2021. **194**: p. 110654.
16. Lalchawimawia, B., et al., *Metal-organic framework-pesticide interactions in water: Present and future perspectives on monitoring, remediation and molecular simulation.* Coordination Chemistry Reviews, 2023. **490**: p. 215214.
17. Kumar, D. and M. Nemiwal, *Applications of Advanced Nanomaterials in Water Treatment*. 2022: CRC Press.
18. Zhou, H.-C., J.R. Long, and O.M. Yaghi, *Introduction to metal–organic frameworks*. 2012, ACS Publications. p. 673-674.
19. Rajesh, R.U., et al., *Metal-organic frameworks: Recent advances in synthesis strategies and applications.* Inorganic Chemistry Communications, 2024. **162**: p. 112223.
20. Abdelhameed, R.M., et al., *Cu–BTC@ cotton composite: design and removal of ethion insecticide from water.* Rsc Advances, 2016. **6**(48): p. 42324-42333.
21. Abdelhameed, R.M. and H.E. Emam, *Modulation of metal organic framework hybrid cotton for efficient sweeping of dyes and pesticides from wastewater.* Sustainable Materials and Technologies, 2022. **31**: p. e00366.
22. Abdelhameed, R., et al., *Kinetic and equilibrium studies on the removal of 14 C-ethion residues from wastewater by copper-based metal–organic framework.* International Journal of Environmental Science and Technology, 2018. **15**: p. 2283-2294.
23. Abdelhameed, R.M., et al., *Zeolitic imidazolate frameworks: Experimental and molecular simulation studies for efficient capture of pesticides from wastewater.* Journal of Environmental Chemical Engineering, 2019. **7**(6): p. 103499.
24. Jamali, A., F. Shemirani, and A. Morsali, *A comparative study of adsorption and removal of organophosphorus insecticides from aqueous solution by Zr-based MOFs.* Journal of Industrial and Engineering Chemistry, 2019. **80**: p. 83-92.
25. Pankajakshan, A., et al., *Water-stable nanoscale zirconium-based metal–organic frameworks for the effective removal of glyphosate from aqueous media.* ACS omega, 2018. **3**(7): p. 7832-7839.
26. Li, W., et al., *In situ preparation of controllable hierarchical pores Zr-PDCs metal–organic frameworks for adsorption of glyphosate.* Chemical Engineering Science, 2024. **288**: p. 119797.
27. Feng, D. and Y. Xia, *Comparisons of glyphosate adsorption properties of different functional Cr-based metal–organic frameworks.* Journal of Separation Science, 2018. **41**(3): p. 732-739.
28. Abdelhameed, R.M., H. Abdel-Gawad, and H.E. Emam, *Macroporous Cu-MOF@ cellulose acetate membrane serviceable in selective removal of dimethoate pesticide from wastewater.* Journal of Environmental Chemical Engineering, 2021. **9**(2): p. 105121.
29. Abdelhameed, R.M., et al., *Amino-functionalized Al-MIL-53 for dimethoate pesticide removal from wastewater and their intermolecular interactions.* Journal of Molecular Liquids, 2021. **327**: p. 114852.
30. Alrefaee, S.H., et al., *Adsorption and effective removal of organophosphorus pesticides from aqueous solution via novel metal-organic framework: Adsorption isotherms, kinetics, and optimization via Box-Behnken design.* Journal of Molecular Liquids, 2023. **384**: p. 122206.
31. NourEldin, B.M., et al., *The behavior of mixed metal based copper–organic framework for uptake of chlorpyrifos pesticide from wastewater and its antimicrobial activity.* Water, Air, & Soil Pollution, 2024. **235**(11): p. 746.

32. Diab, K.E., et al., *Bio-zirconium metal–organic framework regenerable bio-beads for the effective removal of organophosphates from polluted water.* Polymers, 2021. **13**(22): p. 3869.
33. Yousefi, M., et al., *Adsorption of diazinon from aqueous solution using metal organic framework and functionalized graphene: Comparison of BBD, ANN models.* Chemosphere, 2024. **351**: p. 141222.
34. Shadmehr, J., S. Zeinali, and M. Tohidi, *Synthesis of a chromium terephthalate metal organic framework and use as nanoporous adsorbent for removal of diazinon organophosphorus insecticide from aqueous media.* Journal of Dispersion Science and Technology, 2019.
35. Emam, H.E., et al., *Synthesis, spectroscopic study and carbofuran adsorption of mixed metal (Co, Cu)@ Ca-BTC frameworks aimed at wastewater cleaning.* Journal of Industrial and Engineering Chemistry, 2024.
36. Abdelhameed, R.M., et al., *Diazotization-coupling reaction on aluminum-based metal–organic framework for efficient purification of wastewater from carbofuran pesticide.* Environmental Nanotechnology, Monitoring & Management, 2023. **20**: p. 100858.
37. Abdelhameed, R.M., et al., *Effectiveness application of Chitosan/Alginic/Copper–organic framework beads on removal of carbaryl carbamate from wastewater.* Environmental Nanotechnology, Monitoring & Management, 2023. **20**: p. 100832.
38. Qian, K., et al., *Metal–organic frameworks supported surface–imprinted nanoparticles for the sensitive detection of metolcarb*. Biosensors and Bioelectronics, 2016. **79**: p. 359-363.
39. Al-Ahmed, Z.A., *Calcium-organic framework modifiable morphologies for efficient carbamate pesticides adsorption.* Journal of Water Process Engineering, 2025. **70**: p. 107124.
40. Jung, B.K., Z. Hasan, and S.H. Jhung, *Adsorptive removal of 2, 4-dichlorophenoxyacetic acid (2, 4-D) from water with a metal–organic framework.* Chemical engineering journal, 2013. **234**: p. 99-105.
41. Seo, Y.S., N.A. Khan, and S.H. Jhung, *Adsorptive removal of methylchlorophenoxypropionic acid from water with a metal-organic framework.* Chemical Engineering Journal, 2015. **270**: p. 22-27.
42. Elhussein, E.A.A., S. Şahin, and Ş.S. Bayazit, *Preparation of CeO2 nanofibers derived from Ce-BTC metal-organic frameworks and its application on pesticide adsorption.* Journal of Molecular Liquids, 2018. **255**: p. 10-17.
43. Tan, K. and K. Foo, *Preparation of MIL-100 via a novel water-based heatless synthesis technique for the effective remediation of phenoxyacetic acid-based pesticide.* Journal of Environmental Chemical Engineering, 2021. **9**(1): p. 104923.
44. Alsuhaibani, A.M., et al., *Synthesis and characterization of metal–organic frameworks based on thorium for the effective removal of 2, 4-dichlorophenylacetic pesticide from water: batch adsorption and Box-Behnken Design optimization, and evaluation of reusability.* Journal of Molecular Liquids, 2024. **398**: p. 124252.
45. Alaysuy, O., et al., *Synthesis, characterization and adsorption optimization of bimetallic La–Zn metal organic framework for removal of 2, 4-dichlorophenylacetic acid.* Heliyon, 2024. **10**(7).
46. Isiyaka, H.A., et al., *Adsorption of dicamba and MCPA onto MIL-53 (Al) metal–organic framework: Response surface methodology and artificial neural network model studies.* RSC advances, 2020. **10**(70): p. 43213-43224.
47. Liu, B., et al., *Adsorption of 2, 4-dichlorophenoxyacetic acid over Fe–Zr-based metal-organic frameworks: Synthesis, characterization, kinetics, and mechanism studies*. Journal of Environmental Chemical Engineering, 2022. **10**(3): p. 107472.
48. Zhang, Y., et al., *Efficient adsorption removal of 2, 4-dichlorophenoxyacetic acid using amine-functionalized metal–organic frameworks (MOFs): performance and mechanisms.* Separation and Purification Technology, 2024. **334**: p. 126120.
49. Al-Ahmed, Z.A., et al., *Synthesis of magnetic ruthenium metal-organic frameworks for efficient removal of 2, 4-dichlorophenylacetic pesticide from aqueous solutions: Batch adsorption, Box-Behnken design optimization and reusability.* Journal of Water Process Engineering, 2023. **56**: p. 104444.
50. Isiyaka, H.A., et al., *Experimental and modeling of dicamba adsorption in aqueous medium using MIL-101 (Cr) metal-organic framework.* Processes, 2021. **9**(3): p. 419.
51. Huang, B., et al., *Preparation and performance of MOF-808 (Zr-MOF) for the efficient adsorption of phenoxyacetic acid pesticides*. Journal of Industrial and Engineering Chemistry, 2025. **143**: p. 293-302.
52. Zhao, P., et al., *UiO-66: an advanced platform for investigating the influence of functionalization in the adsorption removal of pharmaceutical waste.* Inorganic chemistry, 2019. **58**(13): p. 8787-8792.
53. Zhang, H., et al., *Ce-MOF composite electrospinning as antibacterial adsorbent for the removal of 2, 4-dichlorophenoxyacetic acid.* Chemical Engineering Journal, 2023. **462**: p. 142195.
54. Akpinar, I., et al., *Exploiting π–π interactions to design an efficient sorbent for atrazine removal from water.* ACS applied materials & interfaces, 2019. **11**(6): p. 6097-6103.
55. Akpinar, I. and A.O. Yazaydin, *Adsorption of atrazine from water in metal–organic framework materials*. Journal of Chemical & Engineering Data, 2018. **63**(7): p. 2368-2375.
56. Sakthivel, R., et al., *Cu3 (BTC) 2 metal organic framework as a promising adsorbent for operative exclusion of toxic dyes and herbicide.* Results in Materials, 2024. **21**: p. 100512.
57. Xu, F., et al., *Atrazine removal and in-situ regeneration of molecularly imprinted metal-organic frameworks combined with persulfate.* Inorganic Chemistry Communications, 2025: p. 114169.
58. Isiyaka, H.A., et al., *Effective adsorption of metolachlor herbicide by MIL-53 (Al) metal-organic framework: Optimization, validation and molecular docking simulation studies.* Environmental Nanotechnology, Monitoring & Management, 2022. **18**: p. 100663.

59. Wang, B., et al., *Rapid and efficient removal of acetochlor from environmental water using Cr-MIL-101 sorbent modified with 3, 5-Bis (trifluoromethyl) phenyl isocyanate*. Science of the Total Environment, 2020. **710**: p. 135512.
60. Sakr, M., et al., *Effective removal of acetamiprid and eosin Y by adsorption on pristine and modified MIL-101 (Fe).* Environmental Science and Pollution Research, 2024: p. 1-25.
61. Negro, C., et al., *Highly efficient removal of neonicotinoid insecticides by thioether-based (multivariate) metal–organic frameworks.* ACS Applied Materials & Interfaces, 2021. **13**(24): p. 28424-28432.
62. Singh, S., et al., *CaFu MOF as an efficient adsorbent for simultaneous removal of imidacloprid pesticide and cadmium ions from wastewater.* Chemosphere, 2021. **272**: p. 129648.
63. Xie, L., et al., *Efficient capture of nitrobenzene from waste water using metal–organic frameworks.* Chemical Engineering Journal, 2014. **246**: p. 142-149.
64. Abdelhameed, R.M., et al., *Efficient phenolic compounds adsorption by immobilization of copper-based metal-organic framework anchored polyacrylonitrile/chitosan beads.* International Journal of Biological Macromolecules, 2023. **240**: p. 124498.
65. Lyu, J., et al., *Adsorptive removal of boron by zeolitic imidazolate framework: kinetics, isotherms, thermodynamics, mechanism and recycling.* Separation and Purification Technology, 2017. **187**: p. 67-75.
66. Zhang, J., Y. Cai, and K. Liu, *Extremely effective boron removal from water by stable metal organic framework ZIF-67.* Industrial & Engineering Chemistry Research, 2019. **58**(10): p. 4199-4207.
67. Alkhatib, F., et al., *Efficient removal of deltamethrin from aqueous solutions using a novel lanthanum metal–organic framework: adsorption models and optimization via Box–Behnken design.* ACS omega, 2023. **8**(35): p. 32130-32145.
68. Mogharbel, A.T., et al., *Adsorption and removal of herbicide paraquat from aqueous solutions via novel bimetal organic framework: Kinetics, equilibrium and statistical surface modeling*. Journal of Molecular Liquids, 2024. **414**: p. 126228.
69. Shizari, P.N., et al., *Paraquat herbicide removal from aqueous medium using ZIF-8 and Fe-BTC adsorbents: A comparative study.* Separation and Purification Technology, 2025: p. 132285.
70. Bhadra, B.N., D.K. Yoo, and S.H. Jhung, *Carbon-derived from metal-organic framework MOF-74: A remarkable adsorbent to remove a wide range of contaminants of emerging concern from water.* Applied Surface Science, 2020. **504**: p. 144348.
71. Chang, P.-H., et al., *Novel MOF-808 metal–organic framework as highly efficient adsorbent of perfluorooctane sulfonate in water.* Journal of Colloid and Interface Science, 2022. **623**: p. 627-636.
72. Sakr, M., et al., *Effective removal of acetamiprid and eosin Y by adsorption on pristine and modified MIL-101 (Fe).* Environmental Science and Pollution Research, 2024. **31**(28): p. 41221-41245.
73. Abdelhameed, R., et al., *Kinetic and equilibrium studies on the removal of 14C-ethion residues from wastewater by copper-based metal–organic framework.* International Journal of Environmental Science and Technology, 2018. **15**(11): p. 2283-2294.
74. Xie LiTing, X.L., et al., *Efficient capture of nitrobenzene from waste water using metal-organic frameworks.* 2014.
75. Isiyaka, H., et al., *Experimental and modeling of dicamba adsorption in aqueous medium using MIL-101 (Cr) metal-organic framework. Processes 9: 419*. 2021.
76. Shizari, P.N., et al., *Paraquat herbicide removal from aqueous medium using ZIF-8 and Fe-BTC adsorbents: A comparative study.* Separation and Purification Technology, 2025. **363**: p. 132285.
77. Xu, F., et al., *Atrazine removal and in-situ regeneration of molecularly imprinted metal-organic frameworks combined with persulfate.* Inorganic Chemistry Communications, 2025. **175**: p. 114169.